EUR 4742 e

NEUTRON PROPAGATION
IN WATER-LEAD-IRON LAMINATION

by

B. CHINAGLIA, G. BOSIO, F. VALLANA
(SORIN)
D. MONTI
(FIAT)

(Topical Report)

1972

This report is on sale at the addresses listed on cover page 4

at the price of B.Fr. 85.—

When ordering, please quote the EUR number and the title which are indicated on the cover of each report.

EUR 4742 e

NEUTRON PROPAGATION IN WATER-LEAD-IRON LAMINATION
by B. CHINAGLIA, G. BOSIO, F. VALLANA (SORIN) and D. MONTI
(FIAT)
Topical Report

Neutron propagation in lead-iron-water lamination of various thicknesses has
been accurately investigated by measurements of reaction rates of fast, epithermal
and thermal detectors. A comparison has been made with SABINE and QAD
calculations in order to test their accuracy in dose evaluations. On the basis

of experimental results new approaches to the problem of neutron behaviour
in shields are exposed i.e.
i) the relations between the ratios of reaction rates of the detectors measured
respectively in the configurations and in pure water
ii) methods for calculating neutron spectrum and dose starting from the above
ratios and from the knowledge of a reference spectrum.

EUR 4742 e

NEUTRON PROPAGATION
IN WATER-LEAD-IRON LAMINATION

by

B. CHINAGLIA, G. BOSIO, F. VALLANA
(SORIN)
D. MONTI
(FIAT)

(Topical Report)

1972

ABSTRACT

Neutron propagation in lead-iron-water lamination of various thicknesses has been accurately investigated by measurements of reaction rates of fast, epithermal and thermal detectors. A comparison has been made with SABINE and QAD calculations in order to test their accuracy in dose evaluations. On the basis of experimental results new approaches to the problem of neutron behaviour in shields are exposed i.e.

i) the relations between the ratios of reaction rates of the detectors measured respectively in the configurations and in pure water

ii) methods for calculating neutron spectrum and dose starting from the above ratios and from the knowledge of a reference spectrum.

Index

1. Introduction *)

The primary shield of a reactor for ship propulsion must attenuate neutron and gamma radiation; the materials normally used are water, lead and iron.

The aim of the present work is to give experimental results on thermal, epithermal and fast neutron propagation, useful to describe neutron behaviour in water-lead-iron configurations.

In particular, the following items are developed:

a) verify the calculation methods with respect to the neutron flux attenuation and the energy spectrum;

b) describe the neutron flux (or reaction rate) by some parameters;

c) calculate the neutron spectrum and dose from experimental reaction rates for threshold detectors covering all the energy range.

For item a) we used the following codes: SABINE /1/ a one dimensional removal-diffusion program, QAD-P5 /2/ a three dimensional point kernel code based on Moments Method results for a fission source in homogeneous media. The neutron fast dose calculated by QAD-P5, introducing the removal cross section for lead as a function of hydrogenous material thickness following the lead slab, has been compared with SABINE neutron dose.

Reaction rates measured in the configuration after a 4 cm thick lead plate were analyzed with a method analogous to that reported by Ben-David /3/ in order to obtain the neutron energy spectrum.

---

*) Manuscript received on January 24, 1972

The results of this simple method have been compared with the SABINE spectrum.

For item b) the experimental values in the configurations have been divided by the respective values in pure water to put in evidence the spectral deformation which can be charac terized by some parameters which are a function of metal thick ness.

For item c) a new program named DRR /4/ which computes the neutron dose starting from a reference spectrum and the experi mental results of the detectors has been set up and tested.

The reference spectrum must be known from previous calcula- tions and be near the real spectrum. This method can be useful when a calculation would be difficult, whereas simplified measu rement can be performed, e.g. in an irradiation position within a complex geometry in a strongly heterogeneous composition.

The experiments were made in the shielding facility ETNA of the SORIN swimming pool reactor Avogadro RS1.

2. Experimental apparatus

The neutron source employed in our experiments is a natural U converter plate, 2 cm thick, whose extension is limited by a Boral diaphragm 90 cm in diameter.

A further Boral plate after the source prevents interac- tions of thermal neutrons from the tank water with the source uranium.

The converter plate is placed at the exit of the thermal column of Avogadro RS1 swimming pool reactor, whose power in the course of experiments was 5 MW.

The irradiation facility (ETNA) is of the Lid Tank type composed by a water filled aluminum tank of dimensions $(3x3x2,8)m^3$ (see Fig. 1). Lead and iron shields are located by means of an iron supporting structure (see Fig. 2).

Square lead plates $(1x1)m^2$ are assembled in an iron frame which makes reasonably accurate location possible. Positions for detector foils are obtained by removing lead plugs.

In Fig. 3 a laminated configuration is shown together with a holder and the lead plugs.

The detectors are located along the axis of the configuration and in two transversal positions, by three removable, iron clad holders which avoid dismounting the entire apparatus when detectors are changed.

In water the detectors are positioned by means of small frames, made of steel rods and thin lucite disks fixed to the plates of the configuration.

Foils holders like the above were used in the case of the configuration using pure water, fixed to the iron supporting structure.

The activation detectors used for the various examined energy ranges are described in Tab. I.

In it the activation reaction, the physical shape, the radiation type considered for detection, and the method of counting and of standardization are reported for each detec tor.

Most of the absolute activities have been determined with a calibrated scintillation counter /6/.

Results are given in the form of reaction rates and thermal flux.

Fission chambers were calibrated by means of a method reported in a previous work /5/.

Particular attention has been payed to the perturbation effects produced by the foils themselves. Correction factors have been derived experimentally in all cases, generally by comparison with the response of thin detectors giving negligible perturbation.

3. Experimental results

A) Pure water

The results of measurements performed in pure water are reported in Table II and in Figs. 4 and 5.

B) Metal/water configuration

Three series of shield configurations have been consi dered.

Simple_configurations . A single lead slab (thickness 4 cm or 12.8 cm) is placed in water with its initial face 10 cm from the tank wall.

Composite configurations . A lead slab is sandwiched between two iron plates simulating the supporting structure The whole slab is placed in water at the same distance as above.

Laminar configurations . Several water and lead slabs are arranged in such a way to give volume ratios 2; 1; 0,5.

The examined configurations are listed and labelled in the following Table.

CONFIGURATIONS

Type	Label	Materials (sequence and thickness in cm)
Homogeneous	1	$H_2O(300)$
Simple	2	$H_2O(10) - Pb(4) - H_2O(286)$
	3	$H_2O(10) - Pb(12.8) - H_2O (277.2)$
Composite	4	$H_2O(10) - Fe(1.75) - Pb(4.8) - Fe(2.76) - H_2O(280.7)$
	5	$H_2O(10) - Fe(1.75) - Pb(13.6) - Fe(2.76) - H_2O(271.9)$
Laminar	6	$H_2O(4) - Pb(4) - H_2O(4) - Pb(4) - H_2O(4) - Pb(4) - H_2O(4) - Pb(4) - H_2O(268)$
	7	$H_2O(4) - Pb(8) - H_2O(4) - Pb(8) - H_2O(268)$
	8	$H_2O(8) - Pb(4) - H_2O(8) - Pb(4) - H_2O(8) - Pb(4) - H_2O(264)$

Measurements with at least three detectors:

$$Dy(n,\gamma), \quad Au(n,\gamma)/Cd, \quad Ni(n,p)$$
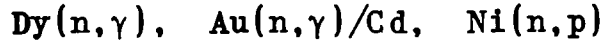
have been made in each configuration. In order to obtain a more complete spectral plot for configurations 1 to 5 the following reactions were also used

$$Np^{237}(n,f), \quad U^{238}(n,f), \quad Rh(n,n')$$

$$In(n,n'), \quad Al(n,p), \quad Al(n,\alpha).$$
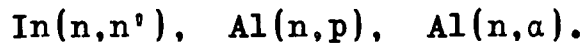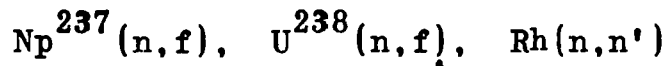
The experimental results are given in Tables III to IX and in Fig. 6 to 14 and are normalized to the same thermal flux incident on the converter, i.e. to the same source power (11 w). The reported errors are those deriving from the count ing statistic. The uncertainty in the absolute values is less than 10% except for Rh (30%) and the Np and U fission chambers (50%).

Errors deriving from the foil position should be less than 10%.

4. Analysis of the experimental results

The experimental results have been plotted in Figs. 15 to 26 as ratios of ρ between the values in the shield configura tion and the corresponding ones in pure water.

In this way the spectral deformations induced by the substitution of water by lead are evidenced and the effects due to geometry or errors in activation cross sections are elimi nated.

From the above graphs the following observations can be made:

- for each detector a peak is found; if the detectors
  are arranged in order of increasing energy: Dy, Au/Cd,
  U-Np-Rh, In, Ni, Al(n,p), Al(n,α), the peak value ρ_{max}
  is continuously decreasing from Au/Cd to Al(n,α) whilst
  its value for Dy is slightly lower than for Au/Cd;

- also the position of the peak is dependent on the energy
  and shifts from about 5 cm behind the slab in water
  towards the interior of the slab with increasing energy;

- the value ρ_t at the rear face of the lead plate decreases
  as the neutron energy increases, except for Dy.

These results clearly indicate that the energy spectrum
in lead is softer than in water. The quantitative increase
of the thermal and epithermal components is approximately
given by the Dy and Au/Cd ratios, and the fast spectrum de-
formation can be deduced by an unfolding procedure of thre-
shold detector data from which a buildup of neutrons below
about 2 MeV is deduced (see for instance Fig. 31 obtained
with the procedure described in Section 6.2).

This behaviour reflects the different scattering and ab-
sorption processes in the two considered media and can be
explained qualitatively considering the changes which occur
in the energy spectrum from an equilibrium shape characte-
ristic of the water medium to a new equilibrium condition
which is not reached however with the lead thicknesses in-
vestigated in the present work. The observed trends are
justified considering that:

- The total cross section is lower for lead than for water in the whole energy range.

- In lead scattering occurs only elastically below ~ 1 MeV and the inelastic fraction is roughly 50% above 4 MeV. Inelastic energy loss is such that most neutrons emerge after collision with an energy in the range (0.5-3)MeV. Since elastic collisions do not change the energy very much, it follows that with respect to water the fast spec trum is enriched below about 2 MeV.

- In the epithermal and thermal range the flux in water resulting from the slowing down of fast neutrons after a sufficient thickness follows approximately the spatial variation of the high energy flux. When the neutrons en ter the lead medium, transfer to lower energy groups is much lower, so that at any energy the spatial variation of the flux is mainly determined by the scattering and ab sorption cross section at the considered energy. Since in addition the relaxation lengths of the low energy neu trons in lead are greater than the relaxation length of the fast leading group in water, the net result is an in crease of ρ in lead.

· The existence and location of the peak is determined respectively by: (1) the lower water albedo for fast neutrons (the peak is inside the slab), (2) the increased slowing down for epithermal neutrons (the peak is at the lead/water boundary), (3) the opposite effects of increas ed absorption and slowed down source for thermal neutrons (the peak is in water).

- The albedo effect is also responsible for the observed
increase of ρ for most detectors before the slab plate.

The dependence of ρ_{max} and ρ_t on the lead slab thickness
t has been plotted in Fig. 27 for Dy, Au/Cd, In, Ni measur-
ed in the simple and composite configurations. In this lat-
ter case ρ_{max} is obtained as

$$\rho_{max} = \rho_{max}^{M}/\rho_{max}^{Fe}$$

where ρ^{M} is the measured value, and ρ^{Fe} is the value of
a single iron plate of thickness equal to the sum of the
iron thicknesses in the experiment, derived from a previous
work /7/.

One can see that the data can be approximated by an ex-
ponential function. This result indicates that the effect
of lead does not depend on the spectrum shape of the inci-
dent radiation (within the range of t investigated) and
one could attempt to describe a laminar configuration start
ing from the ρ curve obtained from a single slab. This has
been done for configuration 6 and Fig. 28 shows the compari
son of ρ's obtained in this way starting from the results
of configuration 2, with the true data obtained directly.
The agreement is rather good and the maximum discrepancy is
observed in some values of Dy reaction rate for which the
true value of ρ_{max} = 5.5 is underestimated by $\sim 30\%$.

5. Comparison with SABINE

A comparison of values of fluxes and reaction rates obtain ed by measurements has been made with those calculated by SABINE, which are reported in the above graphs as continuous lines.

A) Pure water

For what concerns the peak of the thermal flux, calcu-lated values underestimate the experimental ones by 30%, and are then in very good agreement up to 60 cm, reaching a maximum deviation of 30% at 80 cm.

The epithermal flux is underestimated by SABINE every-where, up to a factor of 2 at 80 cm.

Indium reaction rates experimentally measured exceed calculated rates beyond 30 cm from the source, which is justified by a contribution to the reaction (n,n') due to the neutrons produced by reaction (γ,n) on the deuterium contained in water.

No quantitative evaluation of this effect has been how ever attempted since the γ spectrum in ETNA cannot be ac-curately determined due to the complexity of γ sources and shields between the reactor core and the facility.

Rh activation, on the contrary, is in good agreement with calculations.

Experimental results using fission chambers (Np and U) are greater than those expected by calculations by a fac-tor 2, almost constant also for metal-water configurations. It may be presumed that this difference is due to an incor rect standardization of the chambers.

The values of reaction rates of Ni, Al(n,p), Al(n,α) are in agreement (within 20%) with calculations.

B) Configurations

SABINE overestimates thermal fluxes in lead by 30% in a thickness of 4 cm; and by up to a factor 2 within the last plate of laminar configurations.

The epithermal flux is underestimated in pure water but in the lead the calculated values tend to the expe rimental ones at the end of the plate.

Indium activity is always in good agreement with cal- culation, because of the effect of shielding lead on γ rays.

For Rh, Np, U, Ni, Al(n,p) and Al(n,α) the same consi derations as in pure water are valid.

In short, from comparison between experimental and cal culated values, one may say that they agree satisfactory for fast neutrons, but fail somewhat for thermal and epither mal neutrons.

The neutron dose has not been measured directly; how- ever the agreement obtained with the activation detectors may be extrapolated to the dose.

In particular low energy neutrons make a small contribu tion to the dose in water and the discrepancies observed for low energy detectors are of little importance. It is therefore justifiable to consider the SABINE dose as a valid test for assessing the accuracy of other calculation methods described in the next Sections.

6. **Dose calculated by QAD using the removal cross section dependent on the water thickness**

As is well known a point kernel integration program can solve in a simple way problems involving complex geometries. The model used in the QAD code is based on the use of the removal cross sections for evaluating the thickness of the reference material equivalent to the thickness of the various materials in the shield. This procedure is strictly correct only if applied to the same physical configuration used for measuring the removal cross section. In the parti cular case of a slab in water one may expect correct answers (flux or dose predictions) only at points where the equilibrium spectrum in water is re-established (several relaxation lengths behind the slab).

Inside the slab and in the first layer of the following water the removal cross section concept is meaningless; if, as in the case of iron or lead, the removal cross section is greater than $0.1 \frac{cm^2}{g}$ (value commonly used for the reference water medium) the dose in this region will be underestimated by a factor dependent on the slab thickness.

In order to reduce this limitation in the use of QAD a still simple but more realistic procedure has been established, using a removal cross section dependent on the water thickness. Shure /8/ in a previous work has shown that it is possible to define at any point x a cross section $\Sigma_M(x)$ describing the exponential attenuation of a given quantity (the neutron dose) in a material M followed by a water thickness x.

His values, obtained with a multigroup P3MG calculation for iron and lead, approach the known values Σ_M obtained from Lid Tank measurements for a large water thickness.

Therefore an exact description of the neutron dose can be obtained with QAD if a given thickness t of the material is diluted in water in such a way that the total thickness $\bar{t}$ at a point x behind the slab is

$$\bar{t}(x) = t \cdot \Sigma_M(x)/\Sigma_M \qquad (6.1)$$

ranging from a minimum value $\bar{t}(o)$ at the end of the slab to the total value t far from it.

Water behind the slab is therefore divided into a number of regions ending at the points of interest x_1, x_2, ... where a dose calculation is wanted.

A fictitious material density ρ_n is then calculated in each region starting from the slab region $(n = o)$ as follows:

$$\rho_0 = (\rho/t) \cdot \bar{t}(o)$$

$$\rho_1 = (\rho/x_1) \cdot \left[\bar{t}(x_1) - \bar{t}(o)\right] \qquad (6.2)$$

$$\rho_{n+1} = \left[\rho/(x_{n+1} - x_n)\right] \cdot \left[\bar{t}(x_{n+1}) - \bar{t}(x_n)\right]$$

where ρ is the actual material density inside the slab.

This assures that, if the code uses for the material M a constant value Σ_M of its removal cross section, at all the points x_n the relationship:

$$\Sigma_M \left\{ \rho_0 t + \rho_1 x_1 + \rho_2(x_2 - x_1) + \ldots \rho_n(x_n - x_{n-1}) \right\}$$

$$= \rho t \cdot \Sigma_M(x_n) \qquad (6.3)$$

is satisfied.

A similar procedure can also be used for complex lamina tions; in this case the material of a given slab is diluted in all the hydrogeneous regions.

A test of the method has been made using for $\Sigma_M(x)$ the data reported by Shure /8/. Figs. 29 and 30 show two examples relative to metal-water configurations examined in this work. A QAD calculation of the (fast) neutron dose has been made for both the cases of constant and variable Σ_M and the results compared with the SABINE (total) neutron dose.

As shown in the above figures the proposed method gives a rather good description of the dose, whilst the constant Σ_M hypothesis gives large underestimates near the slabs. It must be observed that the absolute values of the dose obtained with SABINE and QAD are somewhat different everywhere because lower energy limits are different for the two codes.

7. Dose calculated from activation detector data

7.1. Outline of the method

In some cases it is possible to obtain experimental data from activation detectors at points of a shield where the spectrum or some integral quantity such as the dose must be known but where accurate calculations cannot be easily performed.

The problem of determining the neutron spectrum starting from the reaction rates of different detectors can be solved by means of different methods based on more or less

sophisticated mathematical treatments of the data. The present accuracy of basic data (cross section) and the cross section versus energy dependence of existing detec tors are such that often solutions without physical mean ing are obtained, unless limiting assumptions are made on the spectrum shape.

The best known methods have been recently reviewed by Bouvard /9/.

The spectrum is described either by functions without a direct physical meaning or by analytical functions which strictly apply only to limited cases (for instance: fission spectrum or modified fission spectrum).

Therefore a common feature is that it is not required (nor possible) to use any information about the spectrum shape, although in many cases it could be possible to have some knowledge derived from calculations or experiments in similar media and geometries.

The method here proposed on the contrary starts from the knowledge of a reference spectrum which is not expected to be very different from the unknown spectrum.

For instance in a heterogeneous shield configuration com posed of several materials M_i it is possible to select one of them, say M_o, to be used as a reference. The effect of the other materials can then be regarded as a perturbation in the homogeneous M_o medium, in which the reference spec-trum $\varphi_o(E)$ can usually be calculated without difficulty.

In the following the method is applied to the laminar lead/water configurations examined in this work, to deter-mine the neutron spectrum and dose.

In this particular case the reference medium is water and the reference spectrum is that existing at the same location in an all water medium. The measured quantities are therefore the ratios ρ reported in Sect. 4.

The use of relative values of ρ instead of absolute reaction rates eliminates the cross section absolute errors.

Other applications of the method are the determination of neutron flux or radiation damage inside experimental faci lities with strong heterogeneities which do not permit an easy prediction. In these cases the reference spectrum is that existing in the homogeneous reactor environment where the facility is inserted.

7.2. Spectrum

The most important features of the method are:

- experimental data are the values of reaction rates in the unknown spectrum $\varphi(E)$ divided by the corresponding quantities in the reference spectrum $\varphi_0(E)$ (ρ ratios)

- each detector i is characterized by a mean energy $E_{i,j}$ dependent on the spectrum $\varphi_j(E)$, which is defin ed as the energy at which the product $\sigma_i(E) \cdot \varphi_j(E)$ reaches its maximum value

- the solution is obtained by an iterative procedure.

This method differs from Ben David's $\underline{/3/}$ approach in the definition of $\bar{E}$ and in the choice of the reference spectrum.

Starting from ρ_i a first estimate Ψ_1 of $\Psi(E) = \varphi(E)/\varphi_0(E)$

is obtained considering

$$\Psi_1(\bar{\bar{E}}_{i,o}) = \rho_i$$

A regular curve $\Psi_1(E)$ is then fitted to the $\Psi_1(\bar{\bar{E}}_{i,o})$ points and a first estimate of $\varphi_1(E) = \Psi_1(E).\varphi_o(E)$ calculated. A new $\bar{\bar{E}}_{i,1}$ value is calculated and the whole procedure repeated until the calculated and measured ρ values are equal within the experimental errors.

An example is given in Fig. 31 relative to the spectrum emergent from a 4 cm lead plate. Detailed shape of the reference spectrum was obtained by a QAD calculation at 18 energies above 0.1 MeV and the procedure was stopped after 5 iterations. The agreement with SABINE is rather good, expecially if one considers that the main interest is not usually knowledge of the exact shape of the spectrum, but rather of the value of some integral quantity which is not very sensitive to small oscillations of $\varphi(E)$.

7.3. DRR method

A different approach is to calculate directly the desired integral quantity A_k (dose, integral flux, radiation damage) starting from a set of N detector responses, A_i (reaction rates per atom).

In the DRR code (Dose from Reaction Rates) the problem has been solved as follows.

The neutron spectrum is divided in N groups whose limits depend on the detectors employed, according to the criteria explained later.

A system of linear equations is then written as:

$$A_i = \sum_{j=1}^{N} \Phi_j \cdot \bar{\sigma}_{i,j} \qquad (i=0,1,\ldots\ldots\ldots N) \qquad (7.1)$$

where:

$$\Phi_j = \int_{E_{j-1}}^{E_j} \varphi(E)\,dE \qquad (7.2)$$

$$\bar{\sigma}_{i,j} = \frac{1}{\Phi_j^o} \int_{E_{j-1}}^{E_j} \varphi(E)\,\sigma_i^o(E)\,dE \qquad (7.3)$$

Starting from the knowledge of the detector responses A_i^o measured in the reference spectrum and A_i in the unknown spectrum, system (7.1) can be written as

$$\rho_i = \sum_j \Psi_j \cdot a_{i,j} \qquad (7.4)$$

in the unknown Ψ_j, where:

$$\rho_i = A_i/A_i^o$$

$$\Psi_j = \Phi_j/\Phi_j^o$$

$$a_{i,j} = \frac{\Phi_j^o \cdot \bar{\sigma}_{i,j}}{A_i^o}$$

By solving this system the required quantity A_k can be calculated by means of the relationships 7.1 and 7.3 with:

$\sigma_k = 1$ if A_k = Total flux above E_o

$\sigma_k = k(E)$ A_k = Neutron dose ($k(E)$ = flux to dose conversion factor)

$\sigma_k = \sigma_D(E)$ A_k = Defect production rate per atom ($\sigma_D(E)$ = cross section for defect production).

An important step for the application of the method is the choice of the detectors and of the energy limits E_j. In each interval a single detector must have a response as prevalent as possible with respect to the others.

From the above principles it follows that the validity of the method is assured if one of the following conditions is ful-filled:

1) the real spectrum is similar in shape to the reference spectrum

2) the dependence of the wanted σ_k upon energy is almost of the same type of that of the various σ_i's mainly in their characteristic field E_{j-1}-E_j ($j = 1$).

In the present form three fast detectors (In, Ni, Al(n,α)) are considered in the DRR code. The fast neutron energy limits satisfying the above condition are given by:

$$\int_{E_o}^{E_1} \sigma_1(E)\varphi^o(E)\,dE = \int_{E_1}^{E_2} \sigma_2(E)\varphi^o(E)\,dE = \int_{E_2}^{E_3} \sigma_3(E)\varphi^o(E)\,dE \qquad (7.5)$$

in addition information about thermal and epithermal flux
is obtained from Dy and Au/Cd.

A complete description of the method is given in /4/
together with the computer program DRR.

An example of the DRR results is given in Fig. 30 which
refers to the dose in the 12.8 cm lead plate configuration.
Comparison with SABINE shows that the dose is underestimat
ed by about 20% in water and up to 50% in lead.

The discrepancy in water and about 50% of it in lead are
due to the different measured and calculated ρ values. In
fact when the SABINE reaction rates are used as inputs these
effects are eliminated.

- In lead the reference spectrum is too different from the
  real spectrum in the epithermal region, and the use of
  a single epithermal detector leads to an underestimate of
  about 20% on the total neutron dose.

8. Conclusions

The principal aim of this work was the determination of the
detailed spatial variation of various activation detector reac
tion rates inside the metal slabs of the lamination considered
and in the surrounding water.

In reactor shielding, when minimum weight or space are requir
ed, the commonly used form of the external part of the biologic-
al shield is a lead barrier followed by hydrogeneous material.

In this case the thicknesses commonly used are in the order
of those investigated in the present work (lead slab up to
12.8 cm, total water thickness behind the slab up to ~ 40 cm)

so that the lack of information for greater thicknesses is of little importance from a practical point of view.

The experimental data have been used first to test the SABINE code. Since the source and shield geometry are well defined and can be accurately described by SABINE, this test is not affected by geometric errors. It has been found that fast neutron detector reaction rates are in excellent agreement, whilst the calculated thermal reaction rate of Dy is overestimated by SABINE in the lead region up to a factor 2. Probably this discrepancy is due to insufficient detail of the spectrum in the thermal region.

The neutron dose is the most important quantity. It has not been measured directly but by the comparison of detector responses. It may be concluded that it is described by SABINE in the investigated region with (better than 20%) reasonable accuracy.

A modification in the use of the point kernel integration code QAD has been proposed. The performed tests indicate that the discrepancies arising from the simplified model used by QAD are greatly reduced in the dose calculation.

Further analysis of the experimental data has permitted description of the perturbing effect of a metal slab in water by means of characteristic ρ versus depth curves for the various activation detectors.

The quantity ρ is the ratio of the reaction rate in the confi guration to that in pure water at the same location. The ρ curves indicate the spectrum softening inside the lead slabs and can be characterized by some parameters.

It may be recalled that the removal cross section definition

is based on the existence of an asymptotic ρ value measured
at a large distance independent of the neutron detector. The
present findings also show that near the slab some relevant
parameters (for instance the peak value) can be approximated
by an exponential function of the metal thickness.

As complementary research, two techniques for the analysis
of experimental data have been developed. The fast neutron
spectrum and the dose can be calculated from the reaction
rates of selected detectors. The methods are rather simple
and with respect to other existing procedures, are based on
the selection of an optimized physical configuration (choice
of detectors, reference spectrum) more than the use of sophi
sticated mathematical procedures.

The methods were tested by comparison with SABINE and sa-
tisfactory agreement was found.

BIBLIOGRAPHY

/1/ C. Ponti, H. Preusch, H. Schubart, "Sabine, a one dimen-
sional bulk shielding program", EUR 3636e (1967)

/2/ R.E. Malefant, "QAD: A series of point kernel general pur
pose shielding programs", LA 3573, Los Alamos Scientific
Laboratories (1966)

/3/ G. Ben-David, E. Nardi, M. Pasternak, "Fast neutron spectro
scopy in a pool-type reactor with activation detectors",
Nucl. Sci. Eng., 20 (1964)

/4/ G. Bosio, F. Cicconi, P.G. Novario, F. Vallana, "Metodo per
il calcolo della dose neutronica in uno schermo, dalle
risposte sperimentali di alcuni rivelatori a soglia",
Programma DRR, Rapporto SORIN F/638 (1970)

/5/ B. Chinaglia, D. Monti, G. Bosio, "Studio della propagazio-
ne neutronica in condotti tubolari con 2 gomiti", Rappor
to SORIN F/433 (1966)

/6/ B. Chinaglia, R. Malvano, Nucl. Instr. & Methods, 45 (1966)

/7/ B. Chinaglia, D. Monti, C. Fedrighini and A.M. Moncassoli,
"Neutron attenuation experiments in iron-water configura
tions", Nucl. Sci. Eng., 27 (1967)

/8/ K. Shure, J.A. O'Brien, D.M. Rothberg (W-BAPL), "Neutron
dose rate attenuation by iron and lead", ASN-CNA TRANS
11 (1968)

/9/ P. Bouvard, Mésure des spectre de neutrons d'energie supé-
rieur à 1 MeV en pile, Note CEA-N-1172 (1969).

TABLE I

·List of detectors

Detectors	Activation reactions	Physical shape	Count ing	Standardization
Dy	$Dy^{164}(n,\gamma)Dy^{165}$	Alloy Al/Dy 10%	β	Comparison with Au
Au/Cd*	$Au^{197}(n,\gamma)Au^{198}$	Pure	γ	(0,411 MeV)
Rh	$Rh^{103}(n,n)Rh^{103m}$	Pure	γ	(20 keV)**
In	$In^{115}(n,n)In^{115m}$	Pure	γ	(0,335 MeV)
Ni	$Ni^{58}(n,p)Co^{58}$	Pure	γ	(0,81 MeV)
Al	$Al^{27}(n,p)Mg^{27}$ $Al^{27}(n,\alpha)Na^{24}$	Pure	γ	(0,84 MeV)
Np	$Np^{237}(n,f)$	Fission chambers		
U	$U^{238}(n,f)$			

*
Cd thickness is 0,5 mm

**Data used: Fluorescent yield of the k shell = 0,78 and
absorption coefficient (20 keV) = 12,5 cm^2/g

All fast neutrons detectors were covered with Cd in order to avoid thermal activations.

TABLE II

Configuration N° 1

Z (cm)	Dy (cm⁻².s⁻¹)	ε%	Au/Cd (s⁻¹.g⁻¹)	ε%	In (s⁻¹.g⁻¹)	ε%	Ni (s⁻¹.g⁻¹)	ε%	Al(n,α) (s⁻¹.g⁻¹)	ε%	Al(n,p) (s⁻¹.g⁻¹)	ε%	Rh (s⁻¹.g⁻¹)	ε%	U (s⁻¹.g⁻¹)	ε%	Np (s⁻¹.g⁻¹)	ε%
0	2,28/7		9,26/6		–		2,02/4		–		–		1,42/5		–		–	
0,15	–		–		3,10/4		–						–		–		–	
0,20	–		–		–		–		3,91/2		2,40/3		–		–		–	
0,60	–		–		–		–				2,25/3		–		–		–	
1	–		–		–		–				–		–		–		1,81/5	
1,1	–		–		–		–						–		2,94/4		–	
2,0	7,0/7		–		–		–						–		–		–	
2,50	–		1,13/7		1,78/4		1,16/4						–		–		–	
3,50	–		–		–		–						–		1,78/4		–	
4,0	8,20/7		–		–		–						–		–		–	
4,70	–		–		–		–						4,40/4	1	–		–	
5,0	–		7,87/6		1,03/4		7,41/3						–		–		7,39/4	
6,0	7,40/7		–		–		–						–		–		–	
7,50	–		4,68/6		6,35/3		4,86/3						–		–		–	
8,0	5,80/7		–		–		–						–		–		–	
8,50	–		–		–		–						–		6,70/3		–	
9,60	–		–		–		–						1,55/4	5	–		–	
10,0	4,20/7		2,64/6		3,90/3		3,28/3		–				–		–		2,55/4	
10,50	–		–		3,60/3		–		9,0/1		–		–		–		–	
10,90	–		–		–		–		–		4,25/2		–		–		–	
12,0	2,80/7		–		–		–		–		–		–		–		–	
13,60	–		–		–		–		–		–		–		2,77/3		–	
14,0	1,90/7		–		–		–		–		–		–		–		–	
14,9	–		–		1,70/3		–		–		–		–		–		–	
15,0	–		7,87/5		1,58/3		1,43/3		–		–		–		–		1,02/4	

Follows Table II (2)

Z (cm)	Dy (cm^{-2}.s^{-1})	ε%	Au/Cd (s^{-1}.g^{-1})	ε%	In (s^{-1}.g^{-1})	ε%	Ni (s^{-1}.g^{-1})	ε%	Al(n,α) (s^{-1}.g^{-1})	ε%	Al(n,p) (s^{-1}.g^{-1})	ε%	Rh (s^{-1}.g^{-1})	ε%	U (s^{-1}.g^{-1})	ε%	Np (s^{-1}.g^{-1})	ε%
16,0	1,30/7		–		–		–		–		–		–		–		–	
18,0	8,50/6		–		–		–		–		–		–		–		–	
18,60	–		–		–		–		–		–		–		1,30/3		–	
19,50	–		–		–		–		–		–		2,98/3	7	–		–	
20,0	5,85/6		2,78/5		–		6,63/2		–		–		–		–		4,37/3	3
20,30	–		–		7,10/2		–		–		–		–		–		–	
20,35	–		–		7,05/2		–		–		–		–		–		–	
20,40	–		–		7,0/2		–		2,50/1	2	–		–		–		–	
22,0	3,80/6		–		–		–		–		–		–		–		–	
23,60	–		–		–		–		–		–		–		5,98/2	3	–	
24,0	2,60/6		–		–		–		–		–		–		–		–	
25,0	–		1,11/5		3,0/2		3,09/2		–		–		–		–		1,97/3	5
26,0	1,72/6		–		–		–		–		–		–		–		–	
28,0	1,19/6		–		–		–		–		–		–		–		–	
28,60	–		–		–		–		–		–		–		2,95/2	5	–	
29,60	–		–		–		–		–		–		6,55/2	13	–		–	
30,0	8,20/5		4,35/4		1,60/2		1,51/2		–		–		–		–		9,30/2	7
30,50	–		–		–		–		7,40/0	5	2,85/1	5	–		–		–	
32,0	5,75/5		–		–		–		–		–		–		–		–	
34,0	4,20/5		–		–		–		–		–		–		–		–	
35,0	–		1,95/4		6,50/1		7,88/1		–		–		–		–		4,55/2	8
36,0	2,90/5		–		–		–		–		–		–		–		–	
36,8	–		–		–		–		–		–		–		9,88/1	5	–	
38,0	2,10/5		–		–		–		–		–		–		–		–	
39,60	–		–		–		–		–		–		1,58/2	18	–		–	

30

Follows Table II (3)

Z (cm)	Dy ($cm^{-2}.s^{-1}$)	ε%	Au/Cd ($s^{-1}.g^{-1}$)	ε%	In ($s^{-1}.g^{-1}$)	ε%	Ni ($s^{-1}.g^{-1}$)	ε%	Al(n,α) ($s^{-1}.g^{-1}$)	ε%	Al(n,p) ($s^{-1}.g^{-1}$)	ε%	Rh ($s^{-1}.g^{-1}$)	ε%	U ($s^{-1}.g^{-1}$)	ε%	Np ($s^{-1}.g^{-1}$)	ε%
40,0	1,60/5		8,94/3		–		3,90/1		–		–		–		–		2,4/2	10
40,3	–		–		4,10/1		–		–		–		–		–		–	
42,0	1,13/5		–		–		–		–		–		–		–		–	
44,0	8,40/4	1	–		–		–		–		–		–		–		–	
45,0	–		4,18/3		–		1,95/1		–		–		–		–		–	
45,2	–		–		1,80/1	8	–		–		–		–		–		–	
46,0	6,20/4	1	–		–		–		–		–		–		–		–	
48,0	4,50/4	2	–		–		–		–		–		–		–		–	
49,60	–		–		–		–		–		–		5,1/1	35	–		–	
50,0	3,40/4	2	2,05/3	5	–		1,03/1	5	–		–		–		–		–	
50,60	–		–		1,04/1	10	–		–		–		–		–		–	
52,0	2,40/4	2	–		–		–		–		–		–		–		–	
54,0	1,80/4	3	–		–		–		–		–		–		–		–	
55,0	–		1,0/3	10	–		–		–		–		–		–		–	
55,50	–		9,4/2	3	6,0/0	25	6,1/0	20	–		–		–		–		–	
56,0	1,38/4	3	–		–		–		–		–		–		–		–	
58,0	1,02/4	3	–		–		–		–		–		–		–		–	
60,0	7,90/3	5	5,9/2	15	–		3,9/0	30	–		–		–		–		–	
60,60	–		–		4,50/0	30	–		–		–		–		–		–	
62,0	6,0/3	5	–		–		–		–		–		–		–		–	
64,00	4,60/3	5	–		–		–		–		–		–		–		–	
65,0	–		2,50/2	6	–		2,5/0	40	–		–		–		–		–	
65,30	–		–		1,30/0	45	–		–		–		–		–		–	
66,0	3,50/3	5	–		–		–		–		–		–		–		–	
68,0	2,60/3	5	–		–		–		–		–		–		–		–	

Follows Table II (4)

Z (cm)	Dy ($cm^{-2}.s^{-1}$)	ε%	Au/Cd ($s^{-1}.g^{-1}$)	ε%	In ($s^{-1}.g^{-1}$)	ε%	Ni ($s^{-1}.g^{-1}$)	ε%	Al(n,α) ($s^{-1}.g^{-1}$)	ε%	Al(n,p) ($s^{-1}.g^{-1}$)	ε%	Rh ($s^{-1}.g^{-1}$)	ε%	U ($s^{-1}.g^{-1}$)	ε%	Np ($s^{-1}.g^{-1}$)	ε%
70,0	2,0/3	5	1,36/2	10	–		8,5/–1	65	–		–		–		–		–	
72,0	1,60/3	5	–		–		–		–		–		–		–		–	
74,0	1,20/3	7	–		–		–		–		–		–		–		–	
75,0	–		6,6/1	10	–		–		–		–		–		–		–	
76,0	9,0/2	7	–		–		–		–		–		–		–		–	
78,0	7,0/2	8	–		–		–		–		–		–		–		–	
80,0	5,5/2	10	4,2/1	12	–		–		–		–		–		–		–	
85,0	–		2,5/1	25	–		–		–		–		–		–		–	
90,40	–·		1,7/1	40	–		–		–		–		–		–		–	

TABLE III

Configuration N° 2

Z (cm)	Dy ($cm^{-2}.s^{-1}$)	ε%	Au/Cd ($s^{-1}.g^{-1}$)	ε%	In ($s^{-1}.g^{-1}$)	ε%	Ni ($s^{-1}.g^{-1}$)	ε%	Al(n,a) ($s^{-1}.g^{-1}$)	ε%	Al(n,p) ($s^{-1}.g^{-1}$)	ε%	Rh ($s^{-1}.g^{-1}$)	ε%	U ($s^{-1}.g^{-1}$)	ε%	Np ($s^{-1}.g^{-1}$)	ε%
0,10	2,23/7		–		–		2,0/4		–		–		1,42/5		–		–	
0,20	–		–		3,10/4		–						–		–		–	
0,40	–		–		–		–		4,20/2		2,35/3		–					
0,75	–		–		–		–		–		–		–		3,05/4		1,80/5	
3,0	7,89/7		1,1/7		–		–		–		–		–		–		–	
4,50	–		8,80/6		–		7,96/3		–		–		–		1,50/4		7,32/4	
5,10	–		–		7,32/3		–		–		–							
5,30	7,87/7		–		–		–		1,90/2		9,87/2		4,20/4		–		–	
7,50	–		4,84/6		–		–		–		–		–		–		–	
7,80	5,55/7		–		–		–		–		–		–					
9,20	–		–		–		–		–		–		–		6,31/3		3,23/4	
9,50	–		–		4,74/3		–		–		–		–		–		–	
9,80	–		–		–		–		1,07/2		4,93/2	1	–		–		–	
9,90	–		2,98/6		–		–		–		–							
10,0	2,71/7		–		–		3,42/3		–		–		1,96/4	2	–		–	
10,50	2,69/7		–		–		–		–		–		–		–		–	
11,0	–		2,50/6		4,34/3		–		–		–		–		–		–	
11,20	–		–		–		3,14/3		–		–		1,90/4	4	–		–	
11,70	2,48/7		–		–		–		8,44/1		3,71/2	2	–		–		–	
12,10	–		–		3,80/3	1	–		–		–		–		–		–	
12,60	2,34/7		–		–		–		–		–		–		–		–	
12,90	–		2,06/6		–		–		–		–		–		–			
13,0	–		–		–		2,52/3		–		–		1,56/4	2	–		–	
14,0	2,27/7		1,53/6		–		1,93/3		–		–		1,22/4	2	–		–	

Follows Table III (2)

Z (cm)	Dy (cm^{-2}.s^{-1})	ε%	Au/Cd (s^{-1}.g^{-1})	ε%	In (s^{-1}.g^{-1})	ε%	Ni (s^{-1}.g^{-1})	ε%	Al(n,α) (s^{-1}.g^{-1})	ε%	Al(n,p) (s^{-1}.g^{-1})	ε%	Rh (s^{-1}.g^{-1})	ε%	U (s^{-1}.g^{-1})	ε%	Np (s^{-1}.g^{-1})	ε%
14,20	–		–		2,70/3	2	–		5,67/1		2,90/2	4	–		–		–	
14,70	–		–		–		–		–		–		–		2,68/3	1	1,40/4	
16,90	–		9,35/5		–		–		–		–		–		–		–	
18,40	–		–		–		–		3,26/1	1	1,40/2	4	–		–		–	
18,70	–		–		9,90/2	2	–		–		–		–		–		–	
18,80	–		–		–		–		–		–		4,26/3	4	–		–	
19,0	1,06/7		–		–		–		–		–		–		–		–	
19,20	–		–		–		7,90/2	1	–		–		–		–		–	
20,0	–		–		–		–		–		–		–		9,80/2	3	4,70/3	1
22,0	–		3,02/5	1	–		–		–		–		–		–		–	
23,70	–		–		4,0/2	3	–		–		–		–		–		–	
23,90	–		–		–		–		–		–		1,705/3	3	–		–	
24,10	3,90/6		–		–		3,62/2	2	–		–		–		–		–	
28,70	–		–		1,80/2	3	–		9,80/0	2	–		–		–		–	
28,90	–		–		–		–		–		–		8,52/2	9	–		–	
29,0	1,45/6		–		–		–		–		–		–		–		–	
29,20	–		–		–		1,84/2	2	–		–		–		–		–	
29,40	–		6,70/4	2	–		–		–		–		–		–		–	
30,0	–		–		–		–		–		–		–		1,90/2	6	8,60/2	2
33,70	–		–		8,70/1	5	–		–		–		–		–		–	
33,90	–		–		–		–		–		–		3,55/2	20	–		–	
34,0	5,70/5	1	–		–		8,80/1	3	–		–		–		–		–	
39,0	2,27/5	1	1,30/4	3	–		–		–		–		–		–		–	
44,0	1,0/5	2	–		–		–		–		–		–		–		–	

TABLE IV

Configuration N° 3

Z (cm)	Dy (cm^{-2}.s^{-1})	ε%	Au/Cd (s^{-1}.g^{-1})	ε%	In (s^{-1}.g^{-1})	ε%	Ni (s^{-1}.g^{-1})	ε%	Al(n,α) (s^{-1}.g^{-1})	ε%	Rh (s^{-1}.g^{-1})	ε%	U (s^{-1}.g^{-1})	ε%	Np (s^{-1}.g^{-1})	ε%
0	1,87/7		–		–		–		–		–		–		–	
0,1	–		8,93/6		3,1/4		–		–		1,42/5		–		–	
0,2	–		–		–		1,91/4		4,0/2		–		–		–	
1,0	–		–		–		–		–		–		3,0/4		1,78/5	
2,4	–		1,20/7		–		–		–		–		–		–	
2,55	–		–		–		1,16/4		–		–		–		–	
3,0	7,76/7		–		–		–		–		–		–		–	
4,2	–		–		–		–		–		–		1,88/4		9,85/4	
4,9	–		9,54/6		–		–		–		–		–		–	
5,0	–		–		–		–		1,96/2		4,60/4		–		–	
5,2	–		–		1,03/4		7,55/3		–		–		–		–	
5,4	8,20/7		–		–		–		–		–		–		–	
7,4	–		6,02/6		–		–		–		2,92/4		–		–	
7,55	–		–		–		4,95/3		–		–		–		–	
7,9	5,85/7		–		–		–		–		–		–		–	
9,2	–		–		–		–		–		–		9,30/3		4,74/4	
9,5	–		–		–		–		1,03/2		–		–		–	
10,0	2,68/7		4,13/6		5,33/3		3,75/3		–		2,24/4		–		–	
11,57	–		3,42/6		–		–		–		–		–		–	
11,60	2,24/7		–		–		–		–		–		–		–	
11,67	–		–		–		3,12/3		–		–		–		–	
11,70	–		–		–		–		–		2,16/4	2	–		–	
13,60	1,81/7		2,84/6		–		2,48/3		–		–		–		–	

Follows Table IV (2)

Z (cm)	Dy (cm^{-2}·s^{-1})	ε%	Au/Cd (s^{-1}·g^{-1})	ε%	In (s^{-1}·g^{-1})	ε%	Ni (s^{-1}·g^{-1})	ε%	Al(n,α) (s^{-1}·g^{-1})	ε%	Rh (s^{-1}·g^{-1})	ε%	U (s^{-1}·g^{-1})	ε%	Np (s^{-1}·g^{-1})	ε%
13,75	−		−		−		−		6,40/1		−		−		−	
14,0	−		−		−		−		−		1,80/4	3	−		−	
14,80	−		−		3,30/3		−		−		−		−		−	
15,43	−		2,38/6		−		−		−		−		−		−	
15,53	−		−		−		1,93/3		−		−		−		−	
15,60	1,62/7		−		−		−		−		−		−		−	
15,80	−		−		−		−		−		1,478/4	4	−		−	
17,60	−		1,96/6		−		1,33/3		−		−		−		−	
18,0	1,52/7		−		−		−		3,65/1		−		−		−	
18,20	−		−		−		−		−		1,08/4	4	−		−	
18,84	−		−		2,08/3		−		−		−		−		−	
22,61	1,13/7		−		−		−		−		−		−		−	
22,80	−		−		1,08/3		−		−		5,0/3	4	−		−	
22,90	−		1,01/6		−		−		−		−		−		−	
23,0	−		−		−		6,07/2		1,65/1	1	−		−		−	
23,5	−		−		−		−		−		−		1,30/3	2	7,7/3	3
27,50	−		3,64/5		−		−		−		−		−		−	
27,70	5,30/6		−		3,53/2		2,54/2		−		−		−		−	
28,0	−		−		−		−		−		1,56/3	5	−		−	
28,50	−		−		−		−		9,70/0	2	−		4,77/2	4	2,26/3	3
32,40	−		1,05/5	1	−		−		−		−		−		−	
32,65	−		−		−		1,20/2	1	−		−		−		−	
32,80	1,81/6		−		−		−		−		−		−		−	

36

Z (cm)	Dy (cm^{-2}.s^{-1})	ε%	Au/Cd (s^{-1}.g^{-1})	ε%	In (s^{-1}.g^{-1})	ε%	Ni (s^{-1}.g^{-1})	ε%	Al(n,α) (s^{-1}.g^{-1})	ε%	Rh (s^{-1}.g^{-1})	ε%	U (s^{-1}.g^{-1})	ε%	Np (s^{-1}.g^{-1})	ε%
32,90	–		–		1,40/2	5	–		–		–		–		–	
33,10	–		–		–		–		–		5,81/2	5	–		–	
33,50	–		–		–		–		4,70/0	2	–		1,85/2	4	8,35/2	13
37,40	–		3,40/4	5	–		–		–		–		–		–	
37,65	–		–		–		5,94/1	2	–		–		–		–	
37,80	6,30/5		–		–		–		–		–		–		–	
38,0	–		–		–		–		–		2,683/2	8	–		–	
38,5	–		–		–		–		–		–		9,73/1	5	3,34/2	6
42,40	–		1,26/4	8	–		–		–		–		–		–	
42,65	–		–		–		2,90/1	3	–		–		–		–	
42,80	2,20/5	1	–		2,70/1	7	–		–		–		–		–	
43,1	–		–		–		–		–		1,279/2	10	–		–	
43,5	–		–		–		–		–		–		3,69/1	10	1,6/2	13
43,8	–		–		–		–		1,39/0	5	–		–		–	
47,30	–		5,26/3	10	–		–		–		–		–		–	
47,60	–		–		–		1,46/1	5	–		–		–		–	
47,80	8,30/4	1	–		–		–		–		–		–		–	
52,30	–		2,22/3	14	–		–		–		–		–		–	
52,70	3,50/4	2	–		5,18/0	10	7,4/0	8	–		–		–		–	
53,5	–		–		–		–		–		–		8,4/0	40	–	
62,7	–		–		1,47/0	20	–		–		–		–		–	

TABLE   V

Configuration N° 4

Z (cm)	Dy (cm^{-2}.s^{-1})	ε%	Au/Cd (s^{-1}.g^{-1})	ε%	In (s^{-1}.g^{-1})	ε%	Ni (s^{-1}.g^{-1})	ε%	Al(n,α) (s^{-1}.g^{-1})	ε%	Rh (s^{-1}.g^{-1})	ε%	U (s^{-1}.g^{-1})	ε%	Np (s^{-1}.g^{-1})	ε%
0,1	–		8,20/6		–		–		–		1,42/5	1	–		–	
0,2	–		–		3,10/4		1,96/4		4,0/2		–		–		–	
1,4	–		–		–		–		–		–		2,83/4		1,83/5	
2,5	6,54/7		–		–		–		–		–		–		–	
4,3	–		–		–		–		–		–		1,50/4		8,67/4	
4,8	–		7,70/6		–		–		2,20/2		–		–		–	
5,0	7,07/7		–		1,039/4		7,71/3		–		4,4/4	2	–		–	
7,3	–		4,79/6		–		–		–		–		–		–	
7,45	–		–		–		5,08/3		–		–		–		–	
7,50	4,94/7		–		–		–		–		–		–		–	
9,25	–		–		–		–		–		–		6,68/3		3,767/4	
9,80	–		3,25/6		–		–		1,016/2		–		–		–	
9,90	–		–		4,68/3		–		–		2,13/4	3	–		–	
10,0	1,24/7		–		–		3,47/3		–		–		–		–	
11,5	–		–		–		2,72/4		–		–		–		–	
11,6	–		2,28/6		3,81/3		–		–		1,775/4	2	–		–	
11,75	4,23/6		–		–		–		–		–		–		–	
13,31	–		–		–		2,10/3		–		1,505/4	2	–		–	
13,51	–		1,78/6		3,19/3		–		5,60/1		–		–		–	
14,03	3,10/6		–		–		–		–		–		–		–	
15,57	2,43/6		–		–		–		–		–		–		–	
16,2	–		–		–		–		4,28/1		1,16/4	2	–		–	
16,35	1,92/6		–		–		–		–		–		–		–	

Follows Table V (2)

Z (cm)	Dy ($cm^{-2} \cdot s^{-1}$)	ε%	Au/Cd ($s^{-1} \cdot g^{-1}$)	ε%	In ($s^{-1} \cdot g^{-1}$)	ε%	Ni ($s^{-1} \cdot g^{-1}$)	ε%	Al(n,a) ($s^{-1} \cdot g^{-1}$)	ε%	Rh ($s^{-1} \cdot g^{-1}$)	ε%	U ($s^{-1} \cdot g^{-1}$)	ε%	Np ($s^{-1} \cdot g^{-1}$)	ε%
16,45	–		1,51/6		–		–		–		–		–		–	
16,70	–		–		2,24/3		1,49/3		–		–		–		–	
19,30	1,92/6		–		–		7,99/2		–		–		–		–	
19,45	–		8,16/5		1,18/3		–		2,25/1		6,0/3	3	–		–	
20,05	–		–		–		–		–		–		1,27/3	1	8,0/3	2
21,80	4,42/6		–		–		4,84/2		–		–		–		–	
22,0	–		5,33/5		–		–		–		–		–		–	
24,0	–		–		–		–		–		2,0/3	5	–		–	
24,30	3,90/6		–		–		3,26/2		1,21/1		–		–		–	
24,50	–		2,97/5		4,18/2		–		–		–		–		–	
27,40	–		–		–		–		–		–		2,89/2	3	1,613/3	5
29,0	–		–		–		–		–		7,0/2	10	–		–	
29,30	1,72/6		–		–		1,49/2		–		–		–		–	
29,50	–		8,61/4		1,70/2		–		–		–		–		–	
29,80	–		–		–		–		5,96/1	3	–		–		–	
34,0	–		–		–		–		–		–		2,62/2	14	–	
34,40	6,10/5		–		8,45/1		7,28/2		–		–		–		–	
34,60	–		2,72/4		–		–		3,33/1	5	–		–		–	
35,80	–		–		–		–		–		–		7,57/1	5	3,63/2	10
39,0	–		–		–		–		–		1,70/2	20	–		–	
39,30	2,13/5		–		–		3,63/1		–		–		–		–	
39,60	–		1,0/4		3,22/1	3	–		–		–		–		–	
44,40	8,46/4	2	–		–		1,89/1	2	–		–		–		–	

Follows Table V (3)

Z (cm)	Dy (cm^{-2}.s^{-1})	ε%	Au/Cd (s^{-1}.g^{-1})	ε%	In (s^{-1}.g^{-1})	ε%	Ni (s^{-1}.g^{-1})	ε%	Al(n,α) (s^{-1}.g^{-1})	ε%	Rh (s^{-1}.g^{-1})	ε%	U (s^{-1}.g^{-1})	ε%	Np (s^{-1}.g^{-1})	ε%
44,70	—		4,22/3		1,43/1	5	—		9,68/−1	10	—		—		—	
45,70	—		—		—		—		—		—		1,54/1	10	—	
48,30	3,66/4	5	—		—		1,11/1	3	—		—		—		—	
48,60	—		1,81/3		—		—		—		—		—		—	
49,0	—		—		—		—		—		2,06/1	75	—		—	
54,30	1,50/4	6	9,51/2	2	4,15/0	10	—		—		—		—		—	
58,30	7,54/3	10	—		—		—		—		—		—		—	
59,40	—		—		—		3,58/0	5	—		—		—		—	
59,60	—		4,25/2	4	—		—		—		—		—		—	
63,30	3,38/3	12	—		—		—		—		—		—		—	
68,30	1,84/3	15	—		—		—		—		—		—		—	

44

TABLE VI

Configuration N° 5

Z (cm)	Dy (cm^{-2}.s^{-1})	ε%	Au/Cd (s^{-1}.g^{-1})	ε%	In (s^{-1}.g^{-1})	ε%	Ni (s^{-1}.g^{-1})	ε%	Al(n,α) (s^{-1}.g^{-1})	ε%	Al(n,p) (s^{-1}.g^{-1})	ε%	Rh (s^{-1}.g^{-1})	ε%	U (s^{-1}.g^{-1})	ε%	Np (s^{-1}.g^{-1})	ε%
0	9,28/6		–		–		–		–		–		–		–		–	
0,1	–		9,50/6		–		–		–		–		–		–		–	
0,2	–		–		3,04/4		1,96/4		–		–		1,40/5	2	–		–	
0,3	–		–		–		–		4,0/2		2,42/3	2	–		–		–	
0,4	–		–		–		–		–		–		–		–		–	
1,1	–		–		–		–		–		–		–		3,01/4		1,71/5	
2,50	6,60/7		1,13/7		–		–		–		–		–		–		–	
4,20	–		–		–		–		–		–		–		1,64/4		8,53/4	
4,90	–		8,80/6		1,10/4		–		–		–		–		–		–	
5,0	7,01/7		–		–		7,48/3		2,04/2		–		4,39/4	2	–		–	
7,50	5,01/7		–		–		–		–		–		–		–		–	
9,30	–		–		–		–		–		–		–		7,23/3	2	3,77/4	2
9,80	–		3,90/6		5,25/3		–		1,02/2	1	5,35/2	2	–		–		–	
10,0	1,28/7		–		–		3,45/3		–		–		2,22/4	3	–		–	
11,50	–		–		–		2,74/3		–		–		1,92/4	3	–		–	
11,60	–		2,90/6		4,50/3		–		8,40/1	2	–		–		–		–	
11,80	5,23/6		–		–		–		–		–		–		–		–	
16,50	–		2,10/6		2,88/3		–		–		–		1,26/4	3	–		–	
16,60	3,68/6		–		–		1,52/3	1	–		–		–		–		–	
18,60	–		1,87/6		–		–		–		–		–		–		–	
19,10	2,71/6		–		–		–		–		–		–		–		–	
19,40	–		–		–		–		2,72/1	3	–		–		–		–	
19,80	–		–		–		–		–		–		9,25/3	3	–		–	

Follows Table VI (2)

Z (cm)	Dy (cm⁻².s⁻¹)	ε%	Au/Cd (s⁻¹.g⁻¹)	ε%	In (s⁻¹.g⁻¹)	ε%	Ni (s⁻¹.g⁻¹)	ε%	Al(n,α) (s⁻¹.g⁻¹)	ε%	Al(n,p) (s⁻¹.g⁻¹)	ε%	Rh (s⁻¹.g⁻¹)	ε%	U (s⁻¹.g⁻¹)	ε%	Np (s⁻¹.g⁻¹)	ε%
20,40	2,27/6		—		—		—		—		—		—		—		—	
20,60	—		1,54/6		1,78/3		9,46/2	2	—		—		—		—		—	
22,50	1,72/6		—		—		—		—		—		—		—		—	
22,70	—		1,34/6		—		—		—		—		—		—		—	
24,40	1,33/6		—		—		—		—		—		—		—		—	
24,90	—		—		—		—		—		—		5,46/3	3	—		—	
25,0	—		—		1,08/3		—		—		—		—		—		—	
25,20	1,02/6		1,11/6		—		—		1,26/1	2	—		—		—		—	
25,50	—		—		—		4,62/2	2	—		—		—		—		—	
28,20	1,17/6		•—		—		2,57/2	2	—		—		2,87/3	3	—		—	
28,30	—		6,0/5		5,22/2		—		7,64/0	5	3,70/1	5	—		—		—	
28,90	—		—		—		—		—		—		—		5,51/2	2	3,50/3	4
30,40	2,64/6		4,13/5		—		—		—		—		—		—		—	
32,80	—		2,40/5	2	1,76/2	5	—		—		—		8,29/2	8	—		—	
33,0	2,25/6		—		—		1,0/2	3	4,24/0	5	—		—		—		—	
33,70	—		—		—		—		—		—		—		2,07/2	6	1,03/3	3
37,70	—		5,90/4	5	6,76/1	10	—		2,28/0	8	—		—		—		—	
38,0	9,60/5		—		—		5,30/1	5	—		—		3,36/2	15	—		—	
38,60	—		—		—		—		—		—		—		7,24/1	10	3,83/2	3
42,80	—		1,61/4	5	2,45/1	13	—		—		—		1,44/2	20	—		—	
4;,0	3,02/5		—		—		2,65/1	10	—		—		—		—		—	
47,80	—		5,6/3	10	1,01/1	30	—		6,36/-1	20	—		8,02/1	20	—		—	
48,0	9,84/4	2	—		—		1,35/1	8	—		—		—		—		—	

42

Follows Table VI (3)

Z (cm)	Dy (cm^{-2}.s^{-1})	ε%	Au/Cd (s^{-1}.g^{-1})	ε%	In (s^{-1}.g^{-1})	ε%	Ni (s^{-1}.g^{-1})	ε%	Al(n,α) (s^{-1}.g^{-1})	ε%	Al(n,p) (s^{-1}.g^{-1})	ε%	Rh (s^{-1}.g^{-1})	ε%	U (s^{-1}.g^{-1})	ε%	Np (s^{-1}.g^{-1})	ε%
48,60	–		–		–		–		–		–		–		1,19/1	25	5,93/1	15
52,80	–		2,1/3	12	4,33/0	50	–		–		–		5,08/1	25	–		–	
53,0	3,48/4	2	–		–		8,55/0	20	–		–		–		–		–	
57,80	–		8,65/2	23	–		–		1,56/–1	30	–		–		–		–	
58,0	1,32/4	3	–		–		6,5/0	15	–		–		–		–		–	
62,70	–		3,85/2	40	–		–		–		–		–		–		–	
63,0	5,54/3	5	–		–		3,33/0	25	–		–		–		–		–	
67,60	–		2,1/2	73	–		–		–		–		–		–		–	
67,80	–		–		–		2,55/0	25	–		–		–		–		–	
68,0	2,69/3	10	–		–		–		–		–		–		–		–	

43

TABLE VII

Configuration N° 6

Z (cm)	Dy (cm^{-2}.s^{-1})	ε %	Au/Cd (s^{-1}.g^{-1})	ε %	Ni (s^{-1}.g^{-1})	ε %
0	2,21/7		1,26/7		2,48/4	
1	5,20/7		1,61/7		2,01/4	
2	6,53/7		1,74/7		1,67/4	
3	6,84/7		1,73/7		1,40/4	
4	5,74/7		1,48/7		1,19/4	
4,55	5,46/7		1,33/7		1,09/4	
5,55	5,30/7		1,20/7		9,62/3	
6,55	5,31/7		1,09/7		8,12/3	
8	5,15/7		9,09/6		6,42/3	
9	5,02/7		8,50/6		5,96/3	
10	4,68/7		7,73/6		4,74/3	
11	4,03/7		6,18/6		3,85/3	
12	2,79/7		4,73/6		3,40/3	
13,25	–		–		2,91/3	
14,25	2,37/7		3,74/6		–	
15,25	–		–		2,20/3	
16	2,18/7		2,82/6		1,82/3	
17	1,91/7		2,25/6		–	
18	1,63/7		1,87/6		1,24/3	
19	1,27/7		1,52/6		–	
20	8,95/6		1,19/6		1,06/3	
21,25	8,22/6		1,08/6		–	
22,25	–		–		7,89/2	
23,25	7,0/6		8,14/5		–	
24	7,0/6		7,04/5		5,40/2	
25	5,9/6		6,04/5		–	
26	5,15/6		4,91/5		3,73/2	1
27	4,26/6		4,15/5		–	
28	3,58/6		3,62/5		3,08/2	1
32	3,12/6	1	2,25/5		1,74/2	1,5
33,5	2,15/6	2	1,59/5		–	
35	1,61/6	4	1,15/5		–	
40	6,15/5	6	3,75/4		5,32/1	3
45	2,09/5	8	1,28/4		–	
50	7,16/4	10	4,95/3	1	–	
55	2,94/4	12	2,02/3	2	–	
60	1,23/4	13	9,68/2	5	–	
65	5,46/3	30	4,82/2	8	–	
70	2,6/3	40	2,1/2	10	–	
75	1,4/3	50	1,1/2	20	–	
80	–		5,5/1	50	–	

TABLE VIII

Configuration N° 7

Z (cm)	Dy ($cm^{-2}.s^{-1}$)	ε %	Au/Cd ($s^{-1}.g^{-1}$)	ε %	Ni ($s^{-1}.g^{-1}$)	ε %
0	2,10/7		1,49/7		2,31/4	
1	4,40/7		1,78/7		1,89/4	
2	6,0/7		1,95/7		1,59/4	
3	6,80/7		1,97/7		1,32/4	
4	4,75/7		1,64/7		1,15/4	
5	4,50/7		1,48/7		1,06/4	
6	4,15/7		1,35/7		9,48/3	
7	3,96/7		1,29/7		8,42/3	
8	3,75/7		1,19/7		7,41/3	
9	3,73/7		1,07/7		6,49/3	
10	3,75/7		9,90/6		5,46/3	
11	3,65/7		8,0/6		4,77/3	
12	3,55/7		7,60/6		3,63/3	
14	3,70/7		5,51/6		2,42/3	
16	2,23/7		4,10/6		1,83/3	
18	1,95/7		3,08/6		1,46/3	
24	1,55/7		1,45/6		6,06/2	2
29	7,70/6		5,10/5		2,45/2	5
34	2,60/6		1,38/5		1,10/2	8
39	8,30/5		4,15/4		5,27/1	9
44	2,55/5		1,42/4	2	2,48/1	12
49	9,0/4	3	5,95/3	5	—	
54	3,52/4	5	2,45/3	8	—	
59	1,50/4	7	1,08/3	9	—	
64	6,95/3	10	5,2/2	10	—	
69	3,3/3	20	3,35/2	15	—	
74	1,8/3	40	1,6/2	30	—	
79	—		5,7/1	40	—	

TABLE IX

Configuration N° 8

Z (cm)	Dy ($cm^{-2}.s^{-1}$)	ε %	Au/Cd ($s^{-1}.g^{-1}$)	ε %	Ni ($s^{-1}.g^{-1}$)	ε %
0	2,95/7		1,36/7		2,16/4	
1	5,50/7		1,55/7		1,81/4	
2	7,50/7		1,64/7		1,47/4	
3	8,60/7		1,50/7		1,20/4	
4	8,54/7		1,30/7		9,74/3	
5	8,30/7		1,18/7		8,23/3	
6	7,25/7		9,50/6		7,06/3	
7	6,20/7		8,10/6		6,06/3	
8	4,30/7		6,50/6		5,39/3	
9	4,06/7		5,30/6		4,62/3	
10	3,55/7		4,55/6		4,13/3	
11	3,45/7		3,70/6		3,54/3	
12	3,25/7		3,40/6		2,85/3	
14	2,68/7		2,50/6		2,11/3	
16	1,90/7		1,55/6		1,46/3	
18	1,24/7		9,70/5		1,03/3	
20	6,50/6		6,70/5		8,24/2	
21	5,80/6		5,30/5		7,33/2	
22	5,40/6		5,00/5		–	
23	–		–		5,21/2	
24	4,75/6		4,0/5		4,48/2	
26	3,55/6		2,95/5		3,56/2	
27,5	2,45/6		–		–	
28	–		1,95/5		2,55/2	
30	1,55/6		1,36/5		1,84/2	
32	8,30/5		8,60/4		1,42/2	3
33	7,20/5		7,60/4		–	
34	6,80/5		–		1,09/2	5
35	6,50/5	3	6,20/4		–	
36	6,18/5	5	5,20/4		8,14/1	6
40	3,75/5	7	2,60/4		4,09/1	10
45	1,55/5	10	9,5/3	2	1,82/1	14
50	6,5/4	10	3,07/3	3	–	
55	2,62/4	12	1,67/3	4	–	
60	1,2/4	15	8,0/2	6	–	
65	5,5/3	16	5,2/2	10	–	
70	2,85/3	18	2,25/2	15	–	
75	1,55/3	25	1,24/2	15	–	
80	7,5/2	25	–		–	
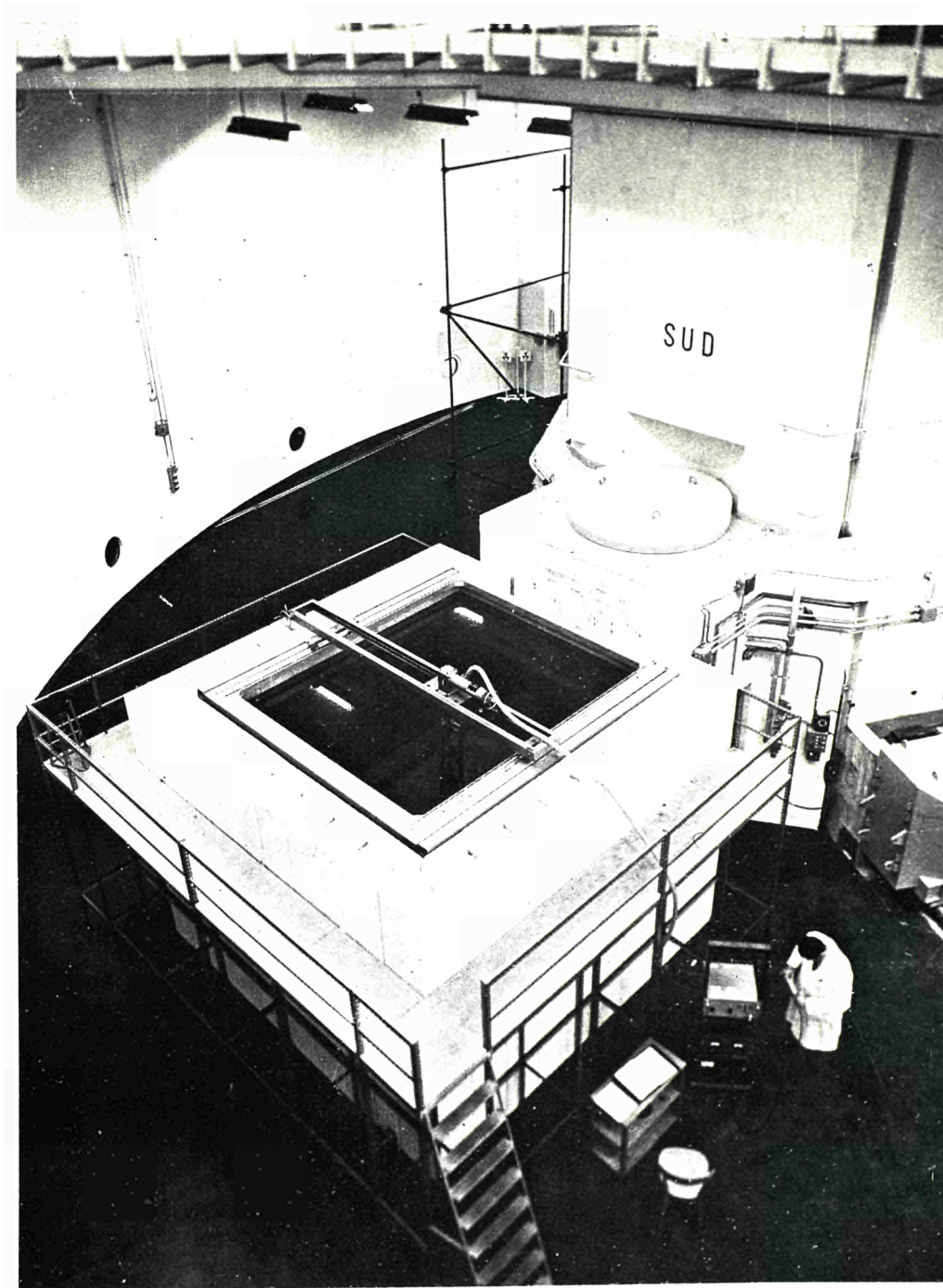
Fig. 1 — ETNA: Irradiation facility.
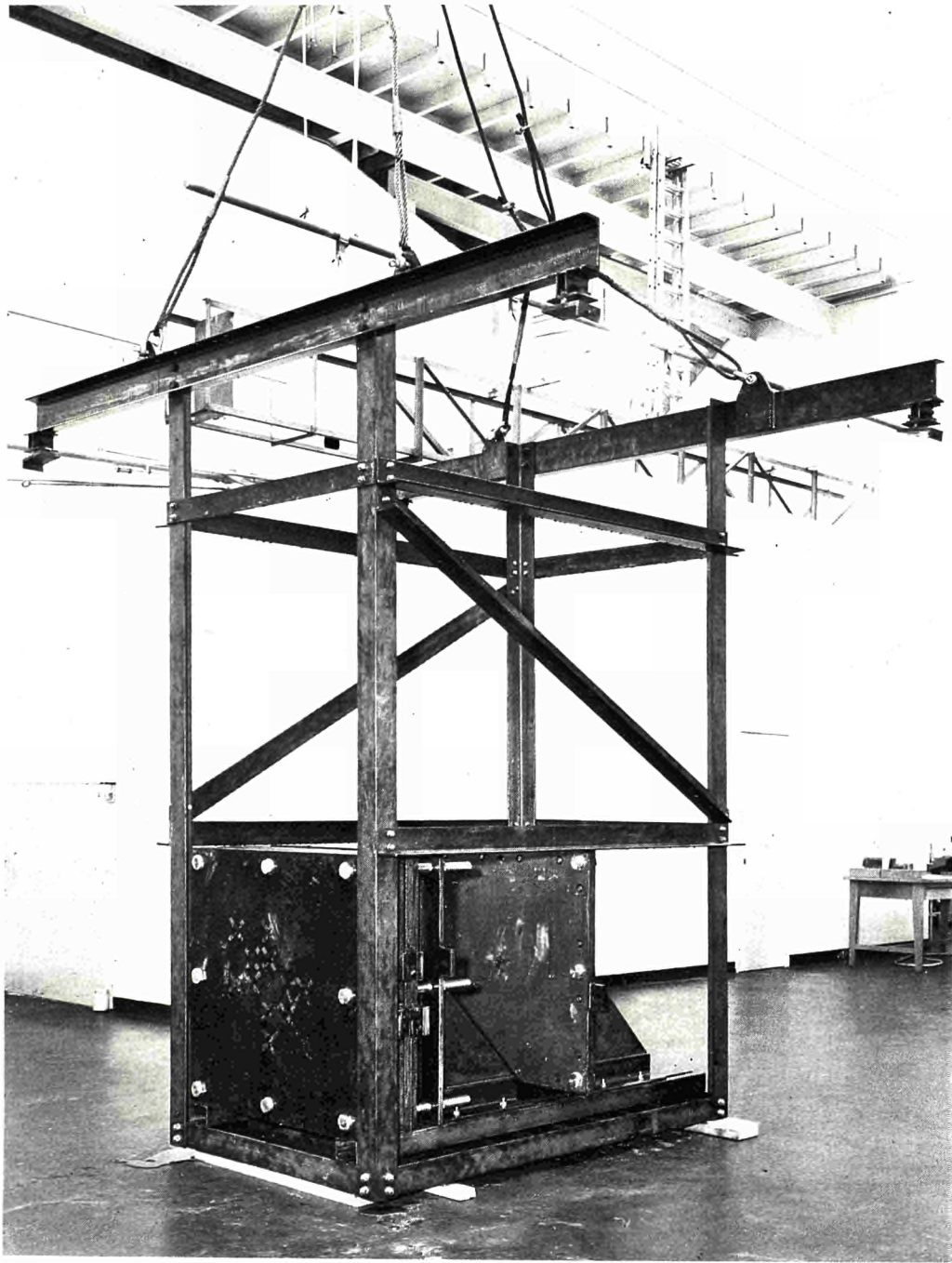
Fig. 2 – View of a configuration on the supporting structure.

Fig. 3 A laminar configuration and a holder with lead plugs.
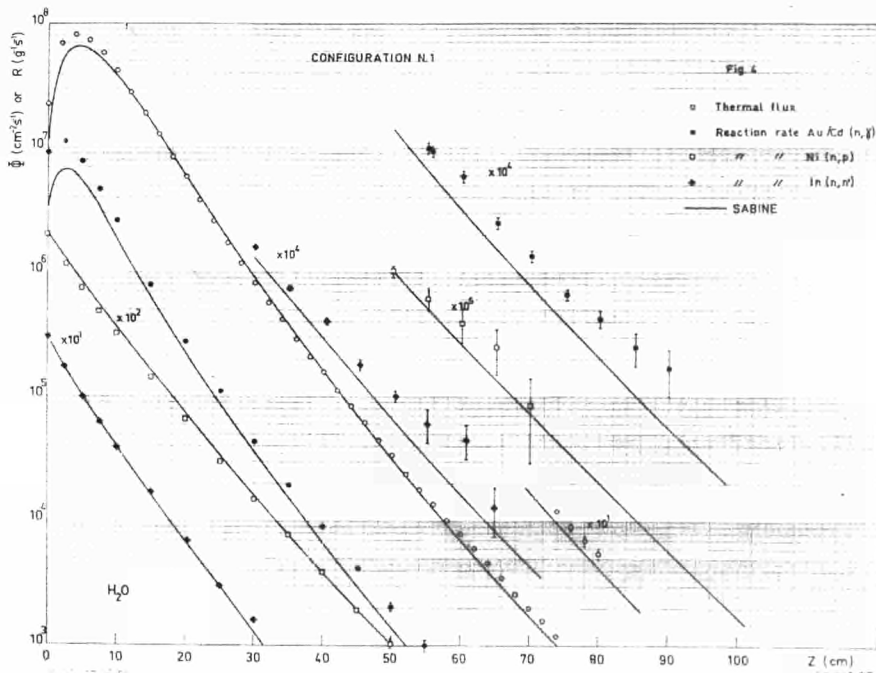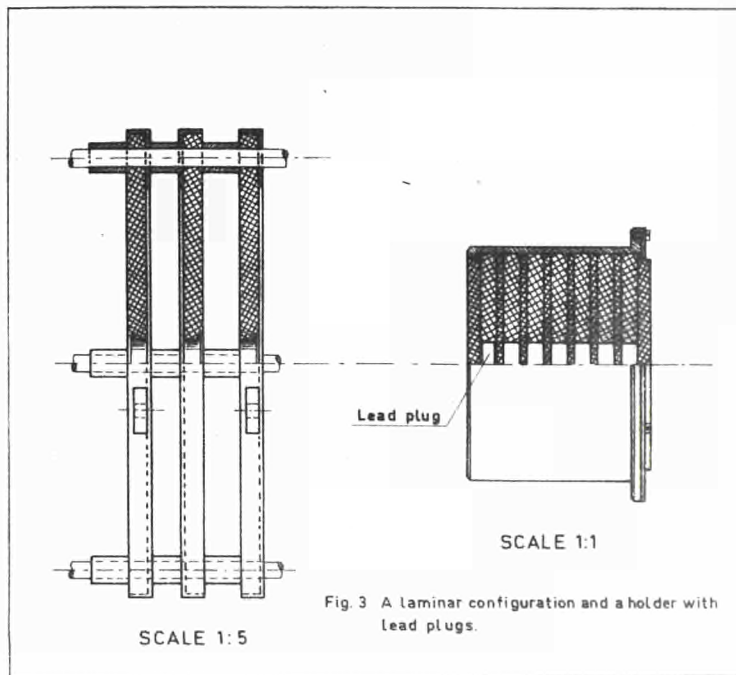
Fig. 4 — Configuration N° 1, flux or reaction rates.
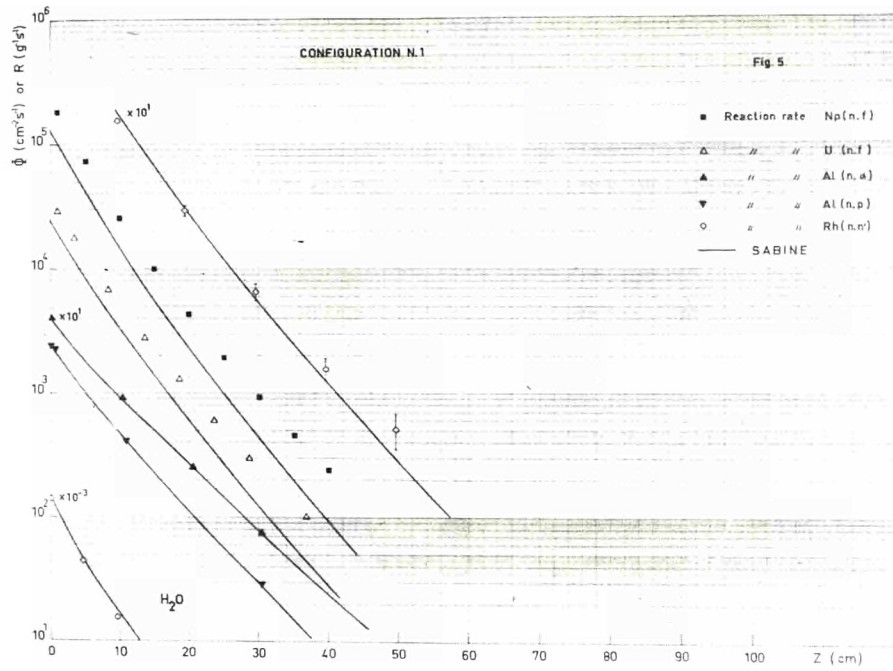
Fig. 5 – Configuration N° 1, flux or reaction rates.
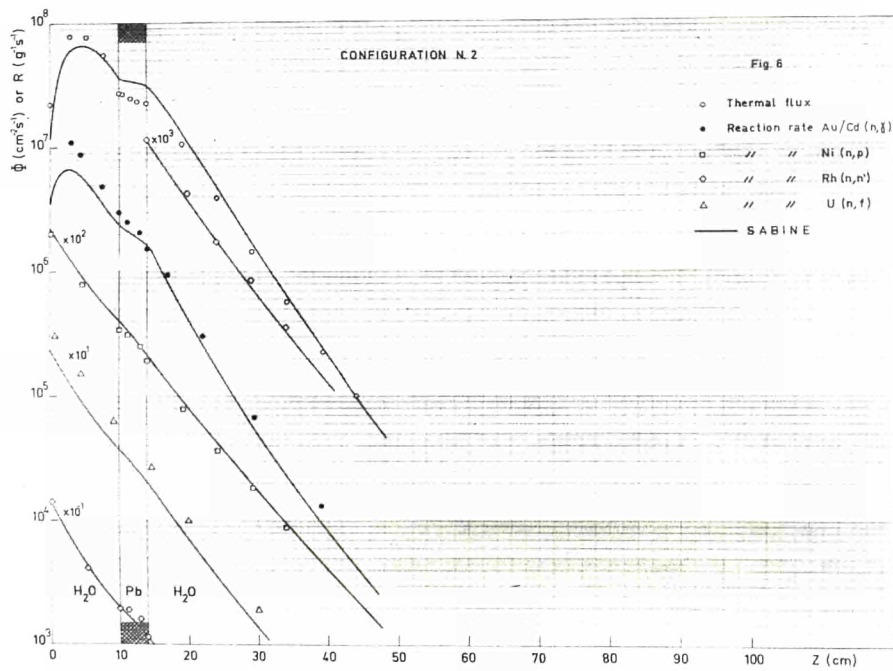
Fig. 6 – Configuration N° 2, flux or reaction rates.
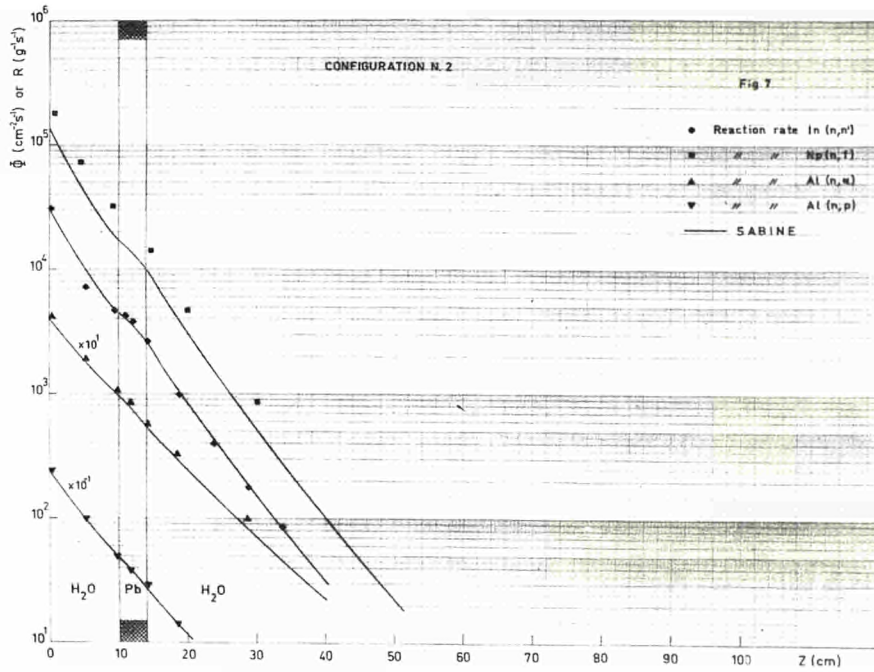
Fig. 7 — Configuration N° 2, flux or reaction rates.
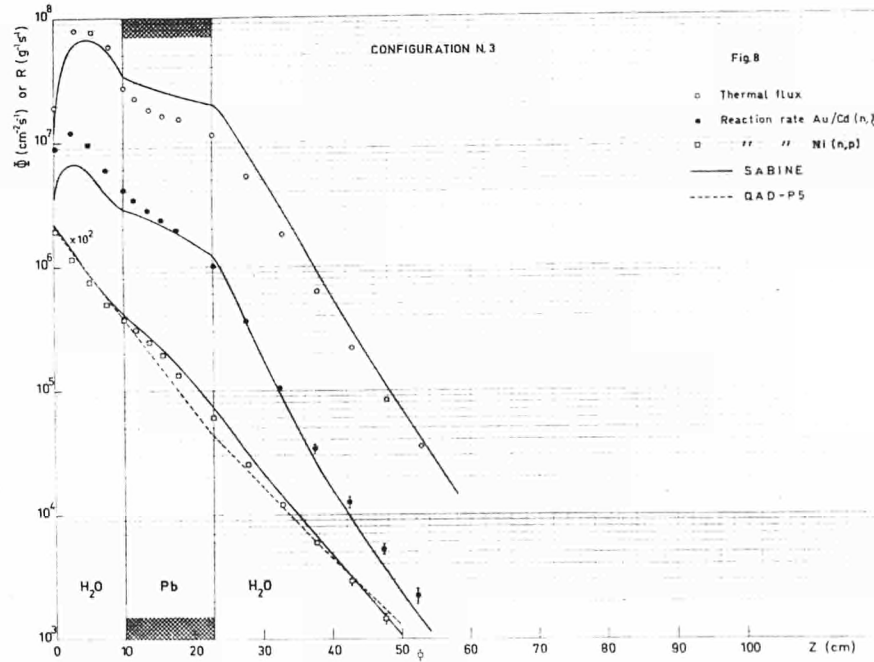
Fig. 8 — Configuration N° 3, flux or reaction rates.
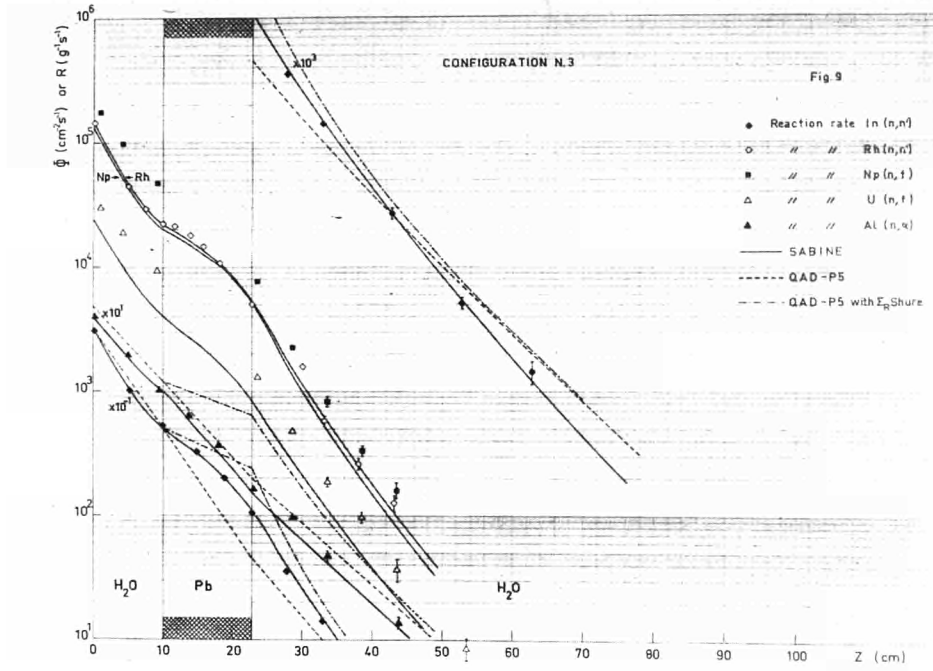
Fig. 9 — Configuration N° 3, flux or reaction rates.
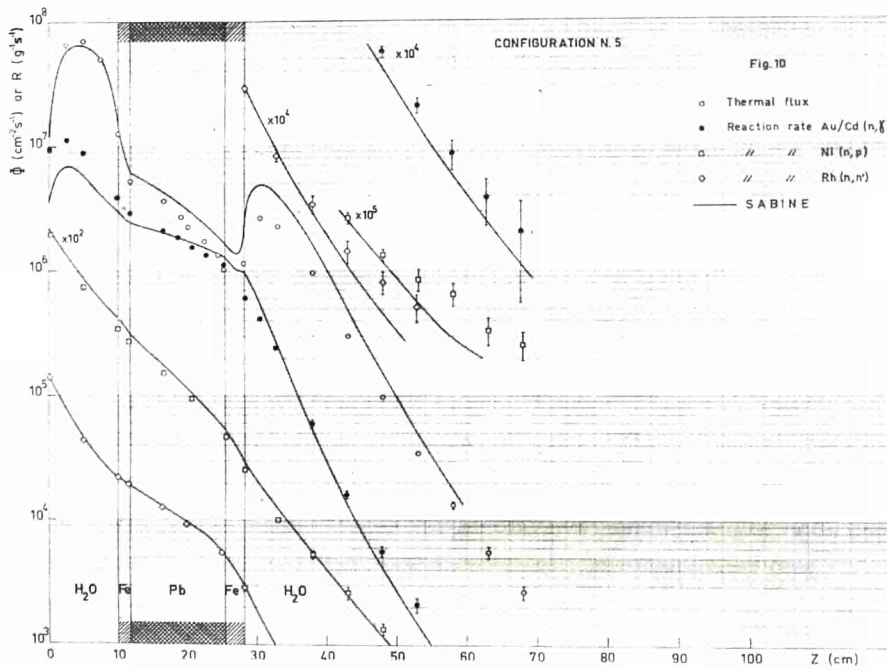
Fig. 10 — Configuration N° 5, flux or reaction rates.
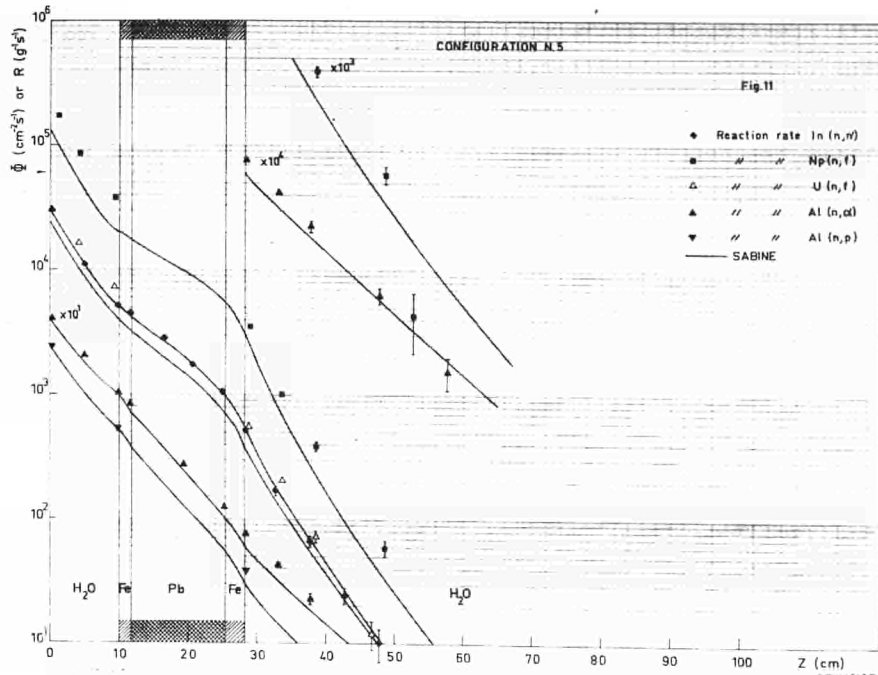
Fig. 11 — Configuration N° 5, flux or reaction rates.
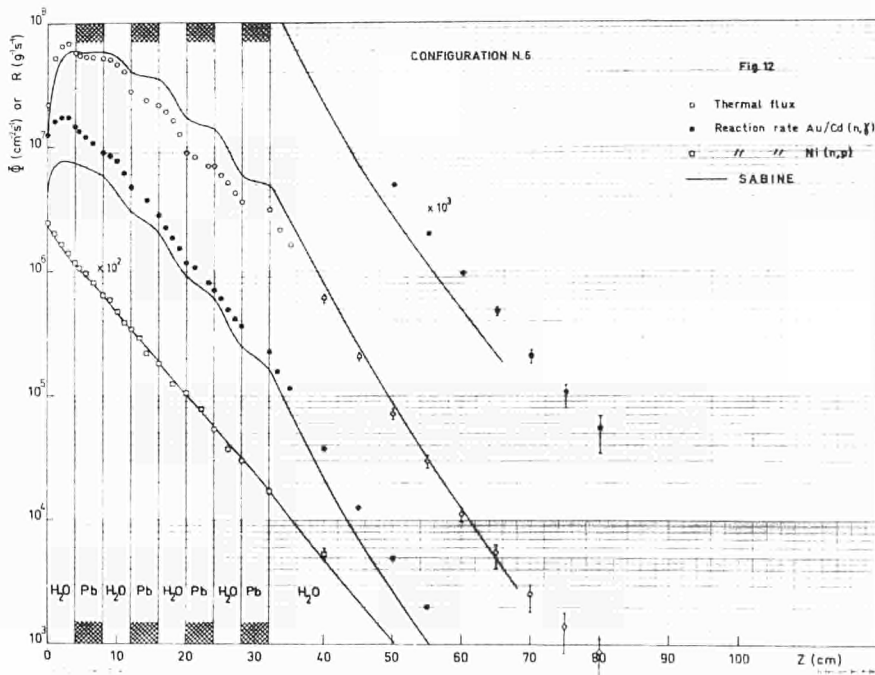
Fig. 12 — Configuration N° 6, flux or reaction rates.
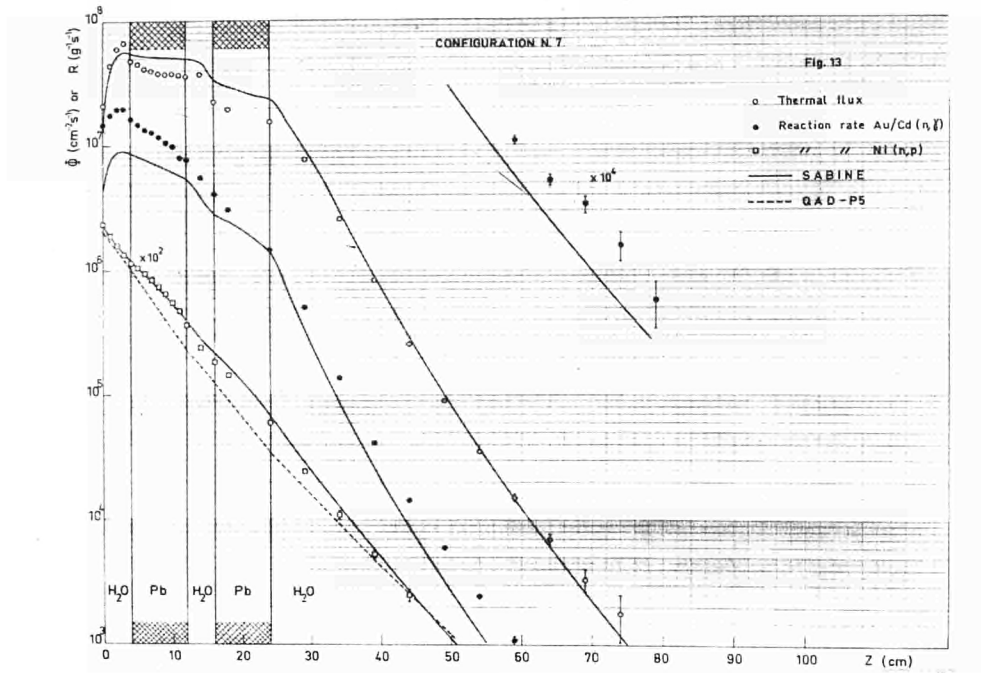
Fig. 13 — Configuration N° 7, flux or reaction rates.
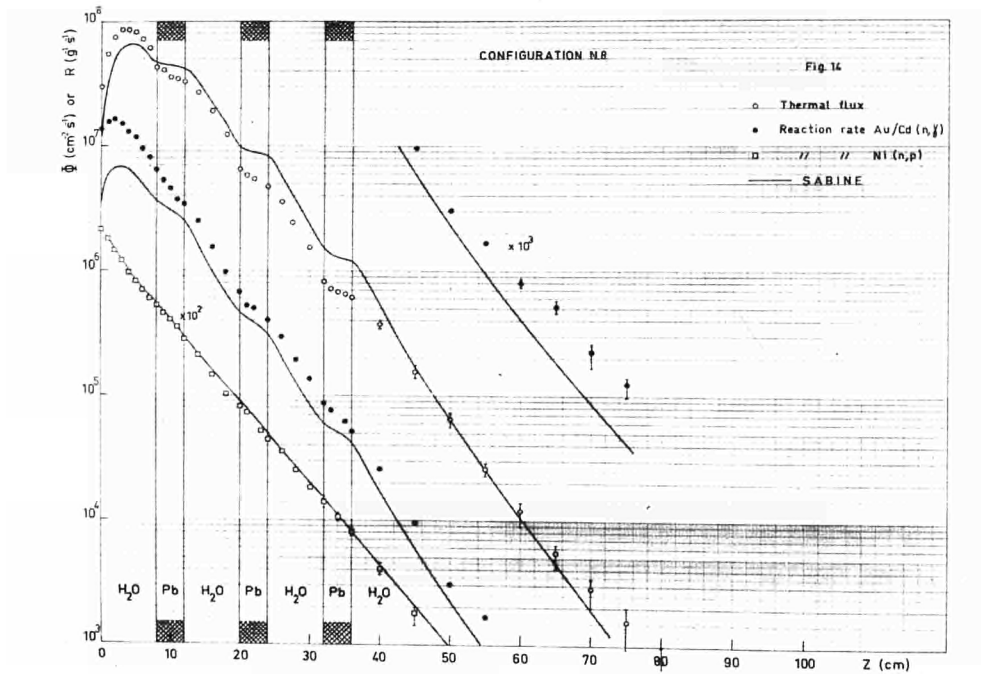
Fig. 14 — Configuration N° 8, flux or reaction rates.
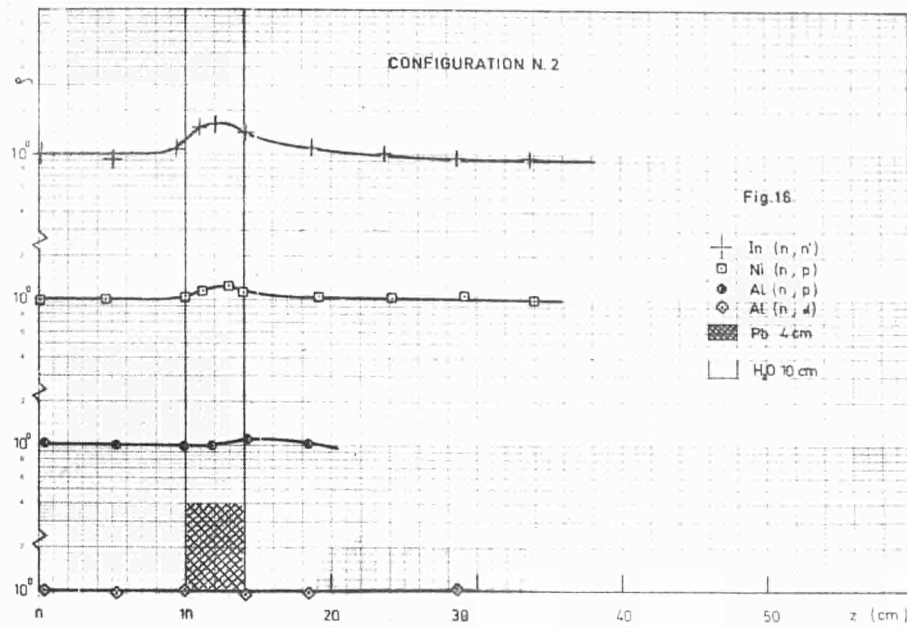
Fig. 15 — Configuration N° 2, ratios ρ, between the values in
the shield configuration and the corresponding ones
in pure water.
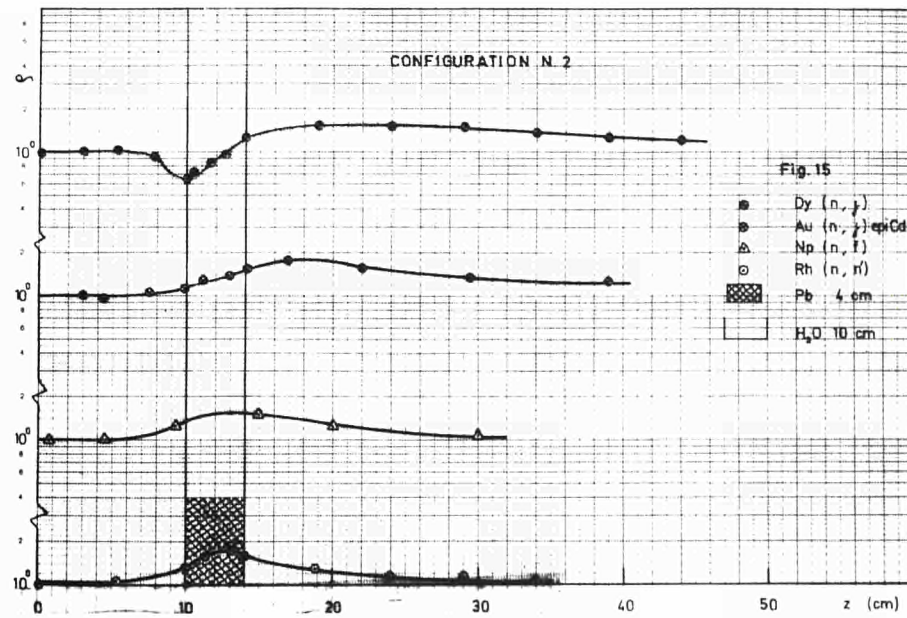
Fig. 16 — Configuration N° 2, ratios ρ, between the values in
the shield configuration and the corresponding ones
in pure water.
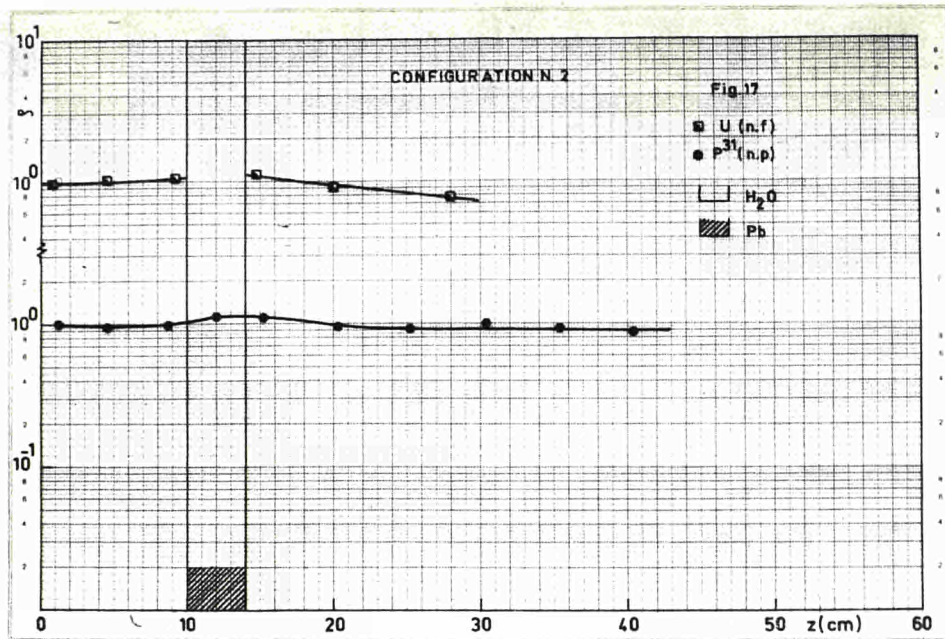
Fig. 17 — Configuration N° 2, ratios ρ, between the values in
the shield configuration and the corresponding ones
in pure water.
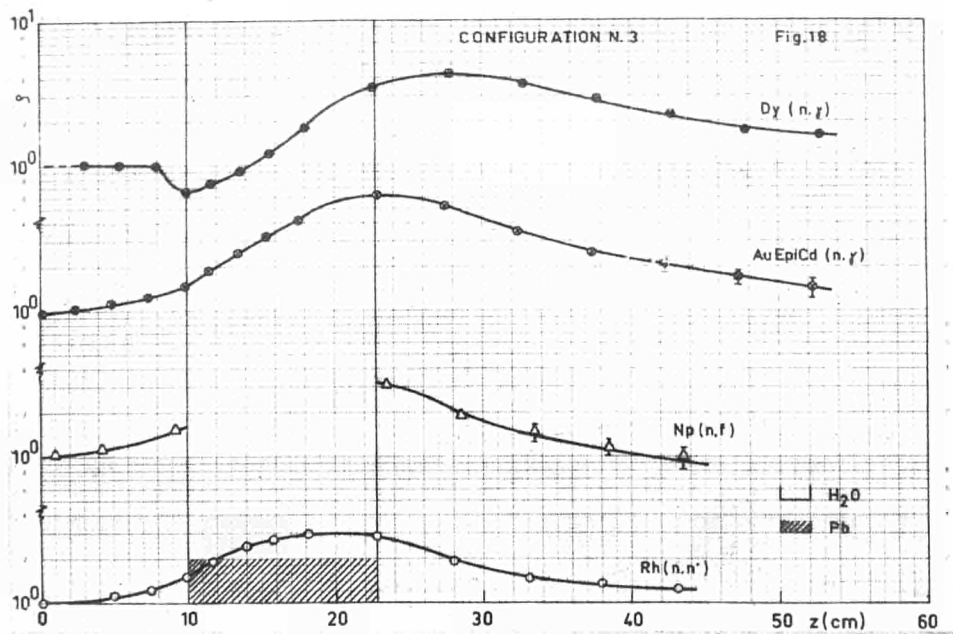
Fig. 18 — Configuration N° 3, ratios ρ, between the values in
the shield configuration and the corresponding ones
in pure water.
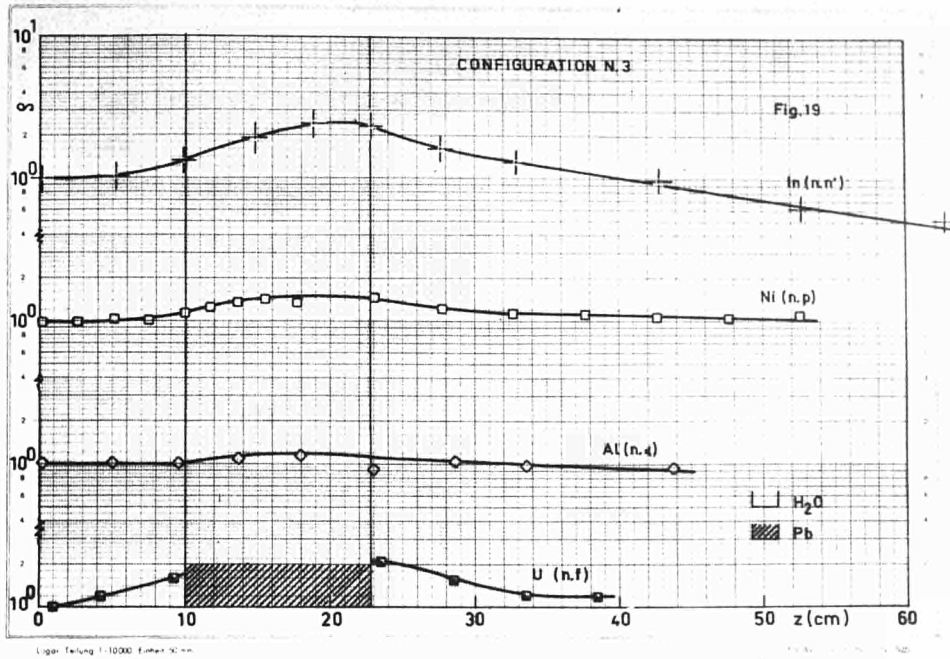
Fig. 19 – Configuration N° 3, ratios ρ, between the values in the shield configuration and the corresponding ones in pure water.
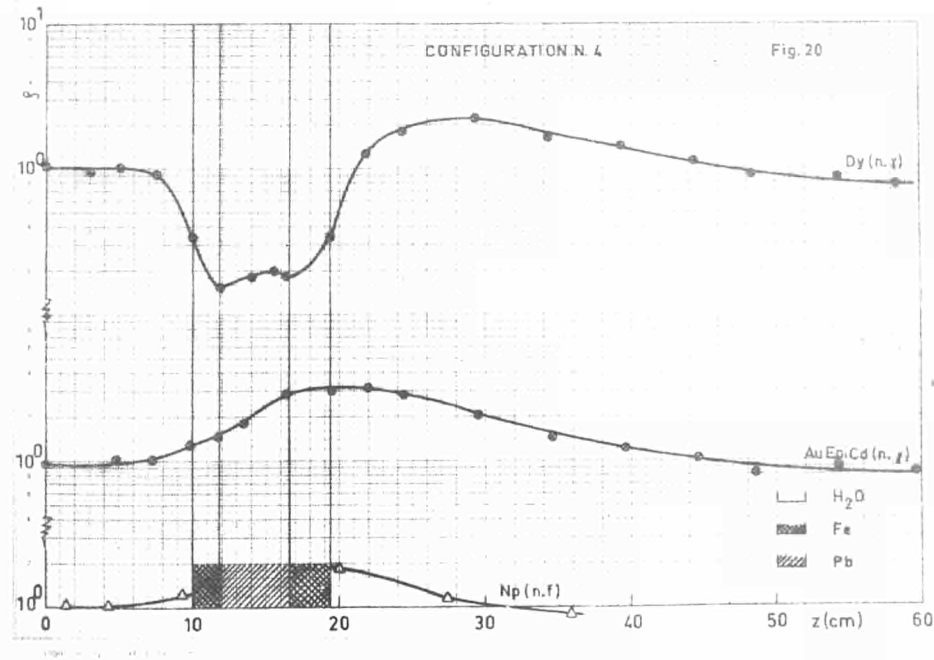
Fig. 20 – Configuration N° 4, ratios ρ, between the values in the shield configuration and the corresponding ones in pure water.
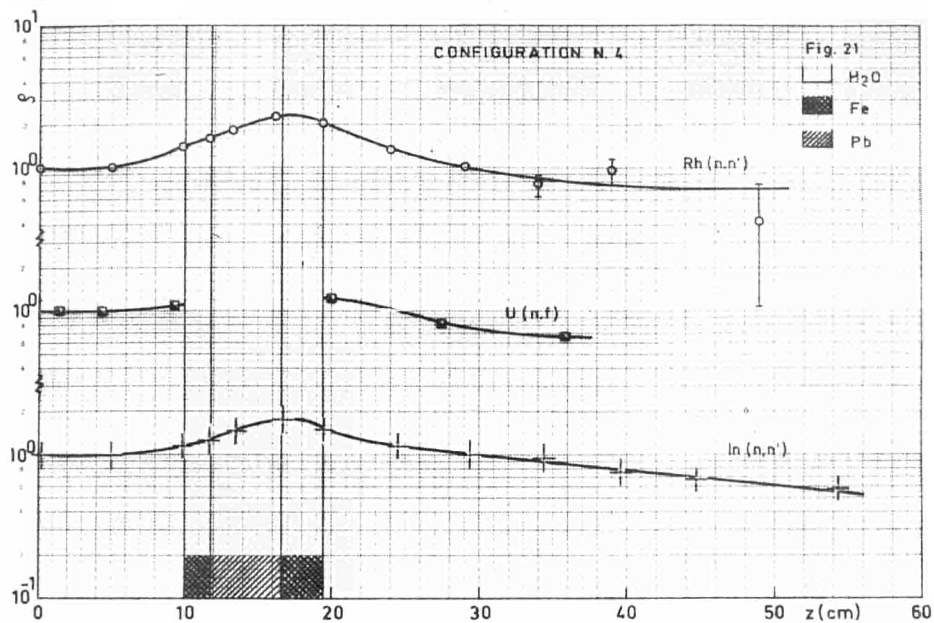
Fig. 21 – Configuration N° 4, ratios ρ, between the values in
the shield configuration and the corresponding ones
in pure water.
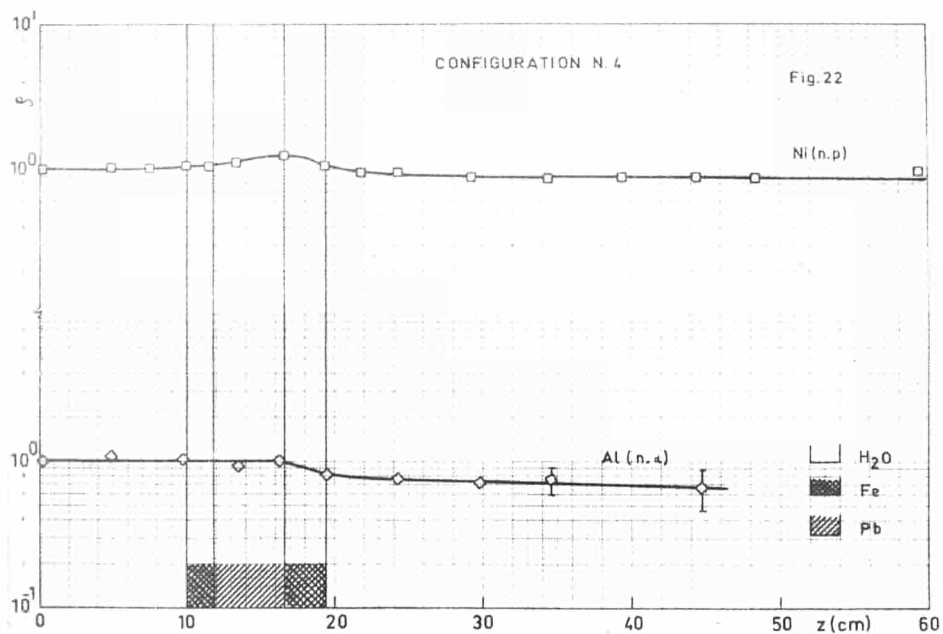
Fig. 22 – Configuration N° 4, ratios ρ, between the values in
the shield configuration and the corresponding ones
in pure water.
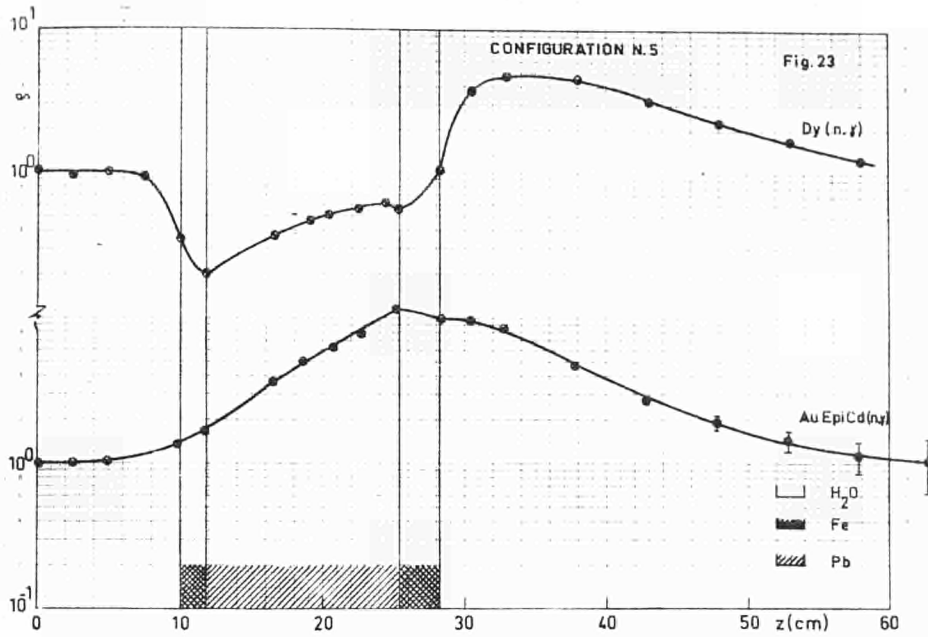
Fig. 23 — Configuration N° 5, ratios ρ, between the values in the shield configuration and the corresponding ones in pure water.
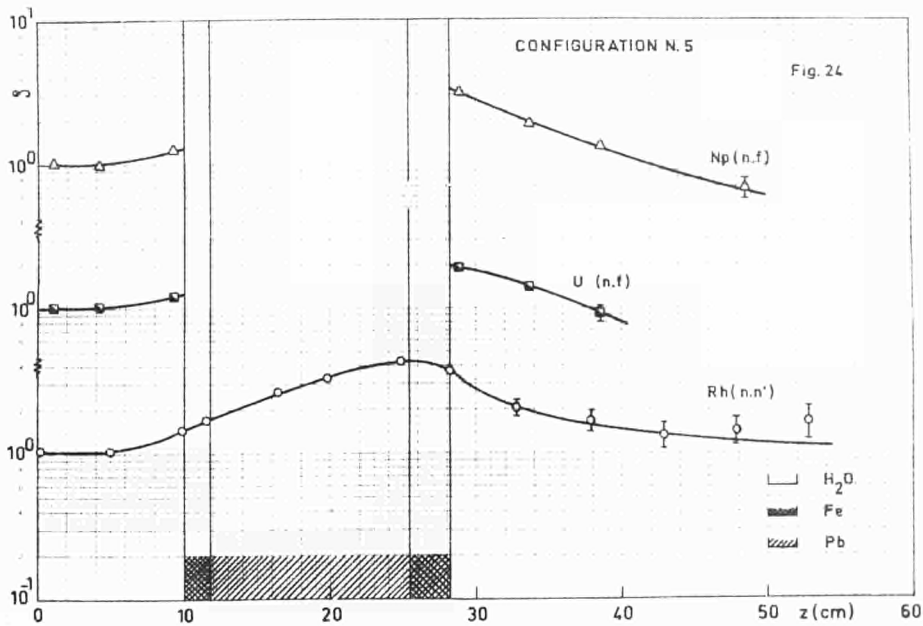
Fig. 24 — Configuration N° 5, ratios ρ, between the values in the shield configuration and the corresponding ones in pure water.
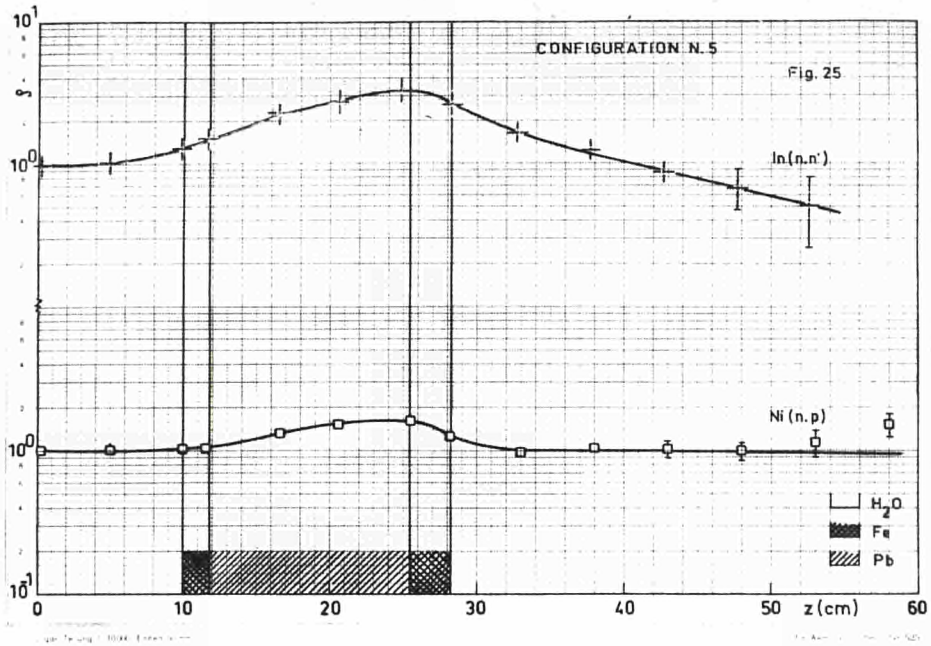
Fig. 25 — Configuration N° 5, ratios ρ, between the values in
the shield configuration and the corresponding ones
in pure water.

Fig. 26 — Configuration N° 5, ratios ρ, between the values in
the shield configuration and the corresponding ones
in pure water.

Fig. 27 — Dependence of ϱ max. and ϱt on the lead slab thickness for Dy, Au/Cd, In, Ni.

○ Dy
● Au/Cd
◆ In
□ Ni

THERMAL FLUX (Dy)

(Au/cd)

(Ni)

Fig. 28 ● } EXPERIMENTAL
         ○ }

———— FROM SIMPLE
        CONFIGURATION
        (4 cm LEAD PLATE)

□ H₂O
▨ Pb
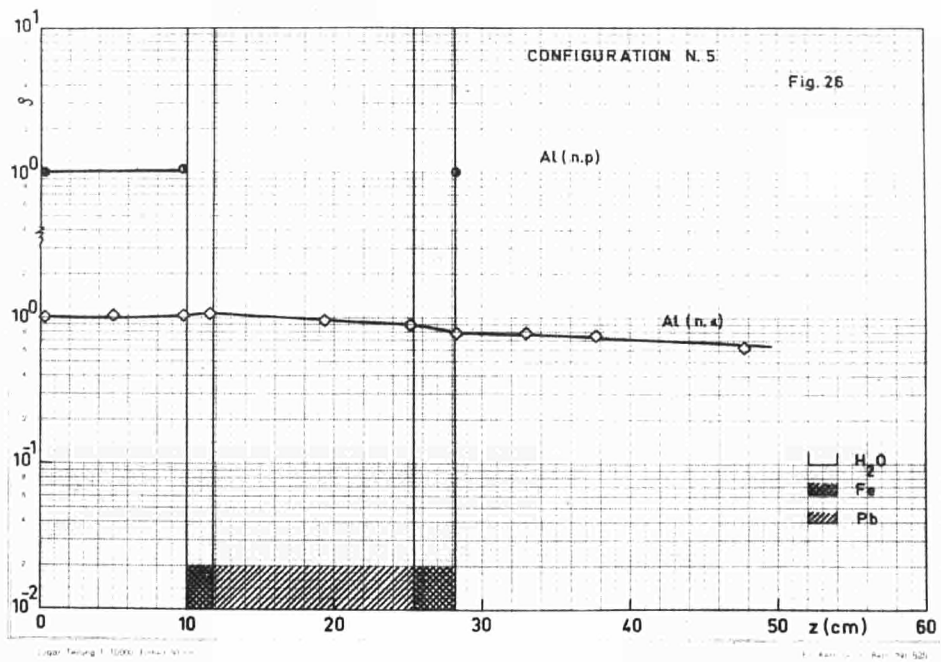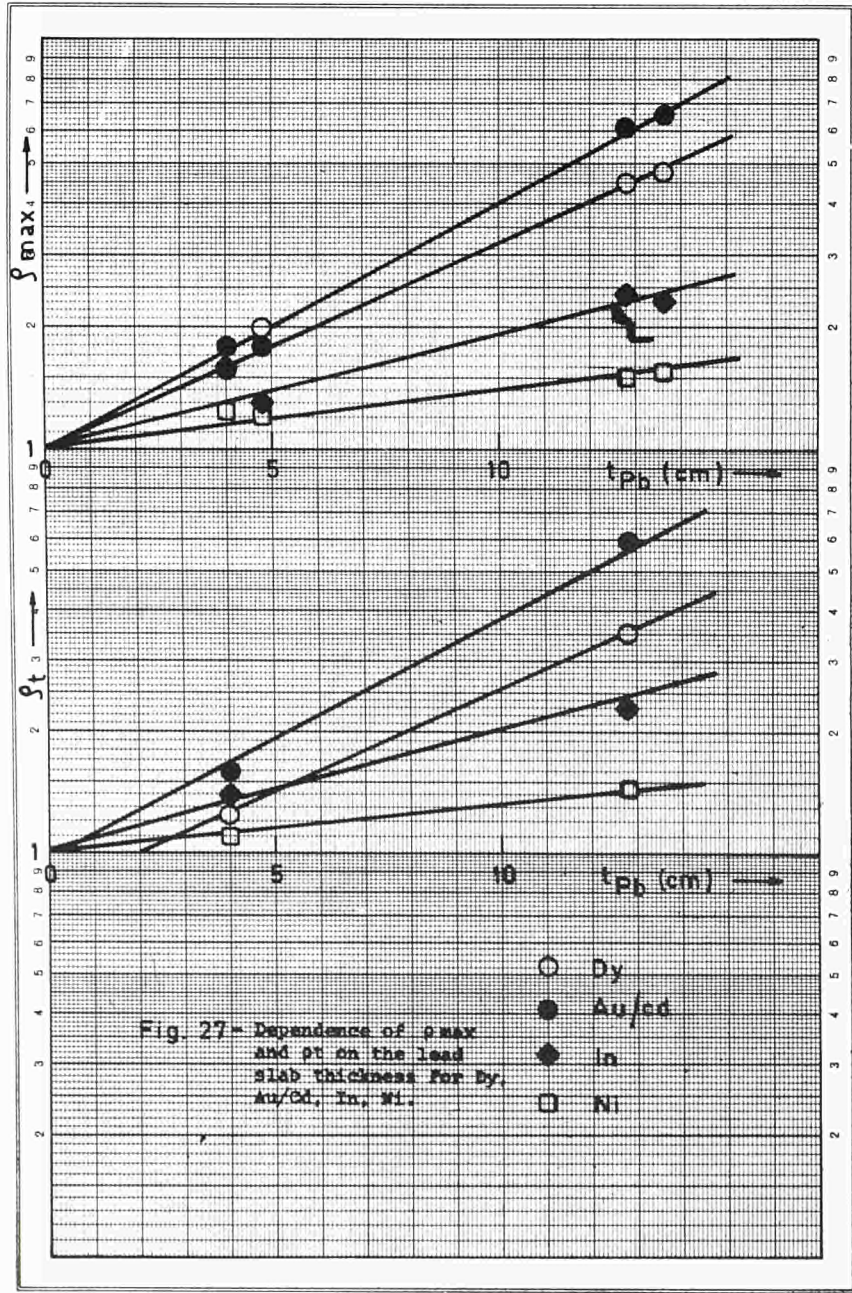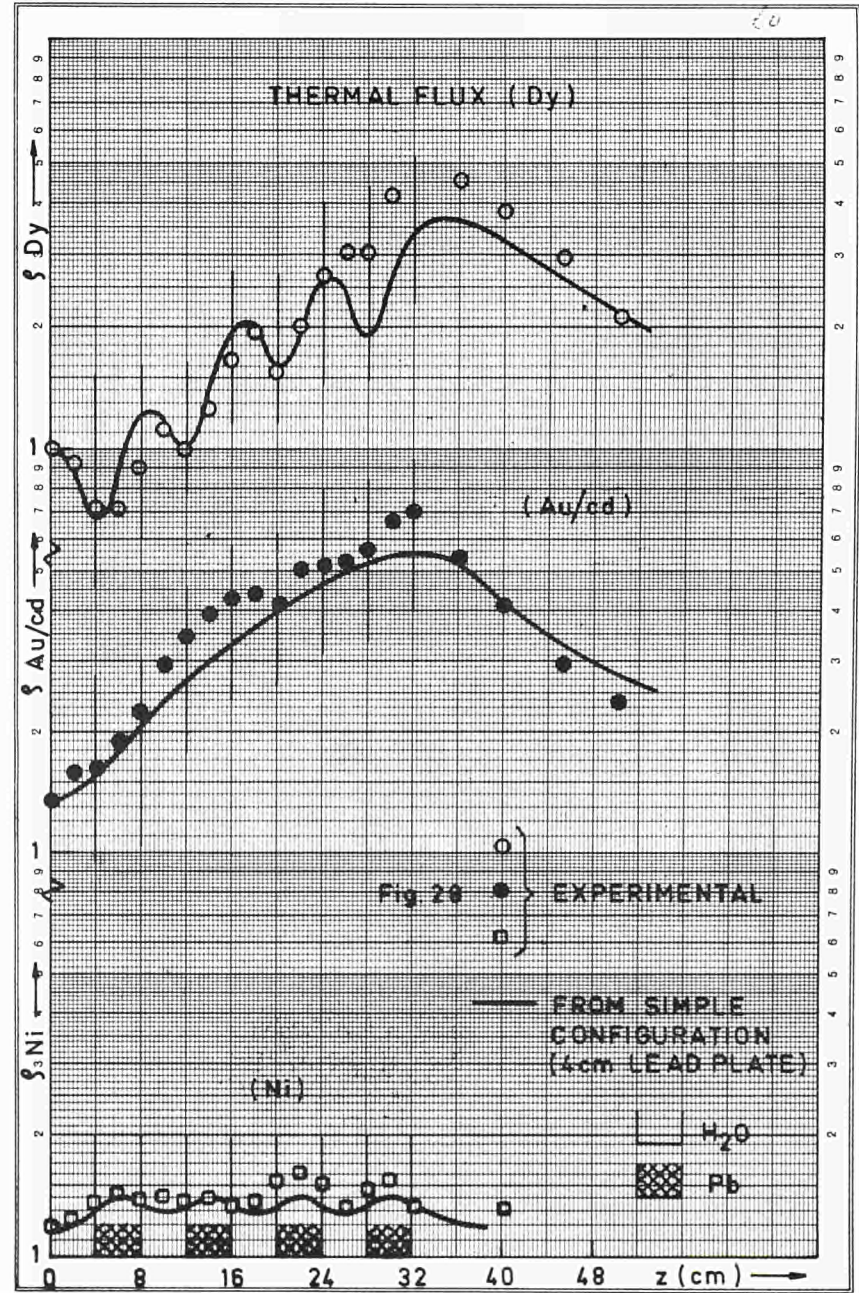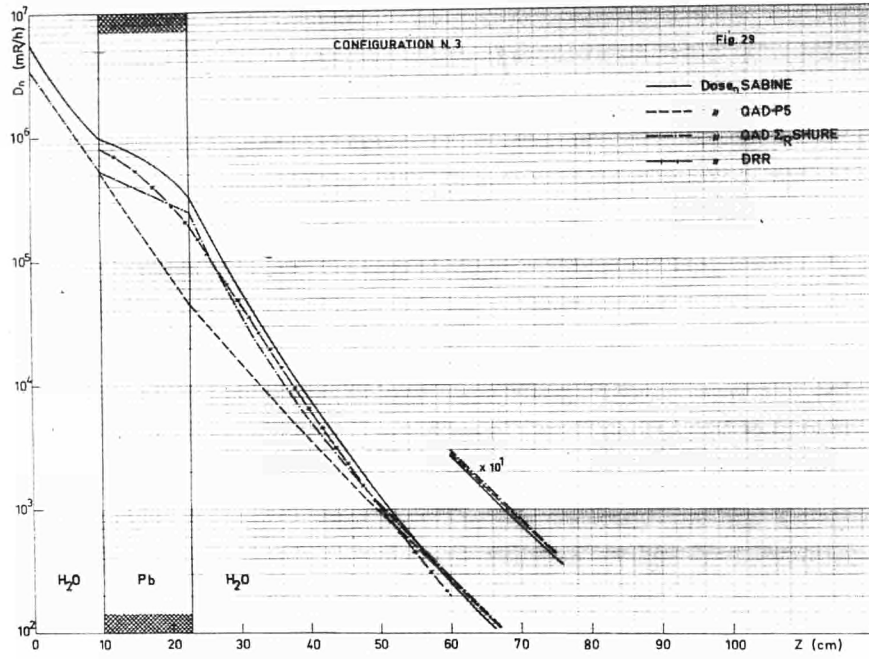
Fig. 29 — Configuration N° 3 calculated doses.
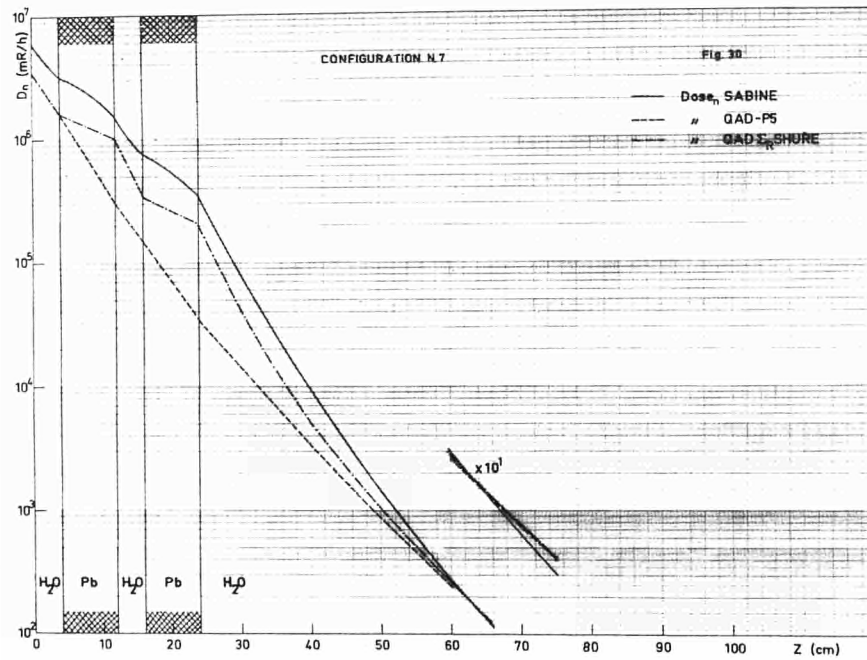
Fig. 30 — Configuration N° 7 calculated doses.
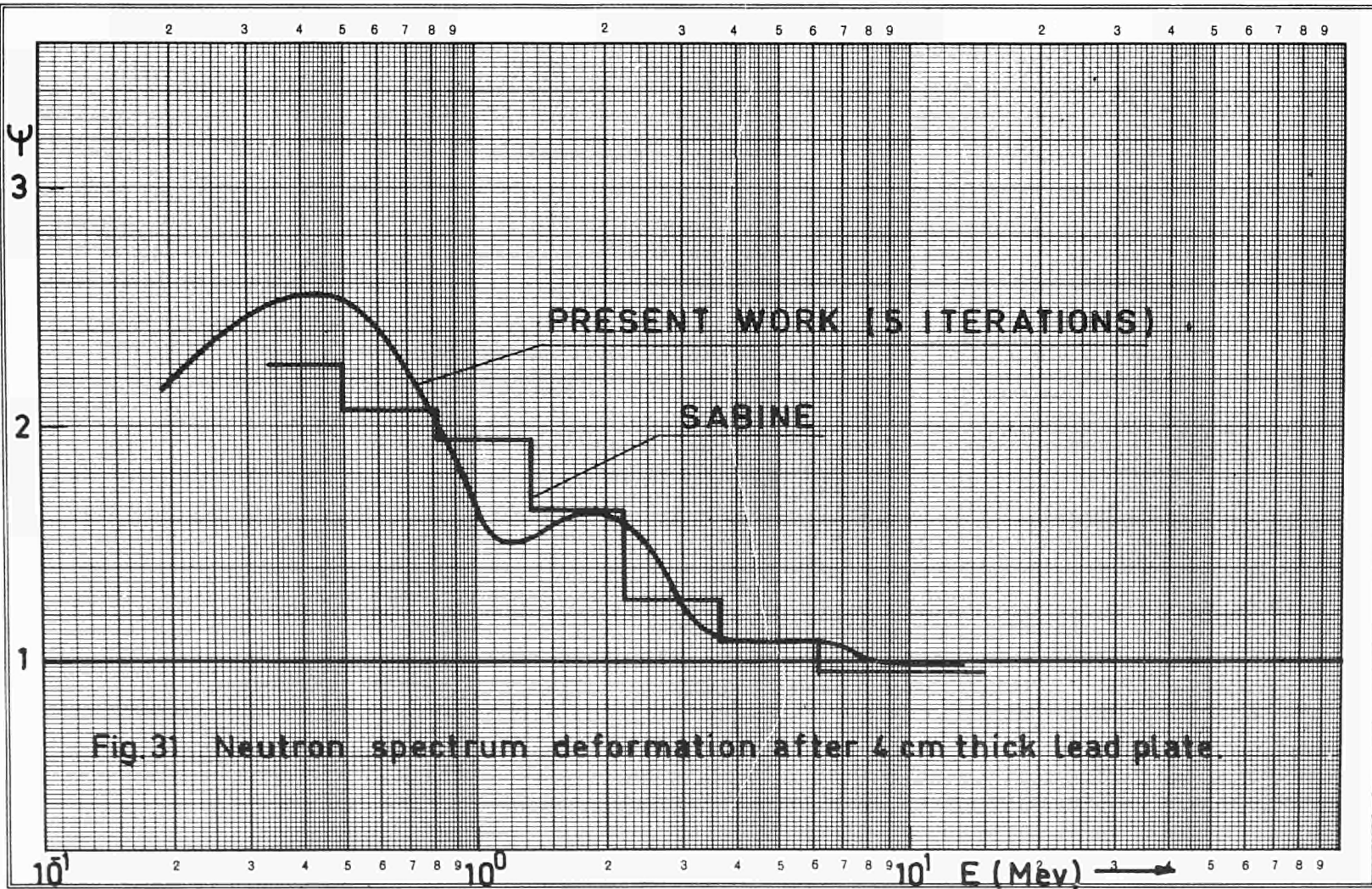
Fig. 31 Neutron spectrum deformation after 4 cm thick lead plate.

Logar. Teilung } 1 - 1000 Einheit } 90 mm
       Division }   Unité }

Ed. Aerni-Leuch, Bern. Nr 534
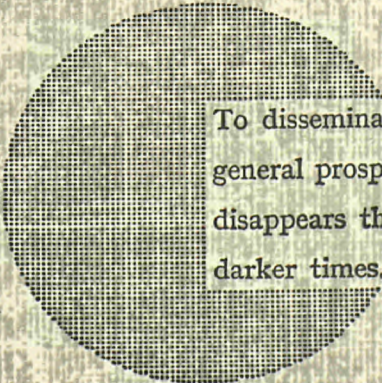
To disseminate knowledge is to disseminate prosperity — I mean general prosperity and not individual riches — and with prosperity disappears the greater part of the evil which is our heritage from darker times.

Alfred Nobel

SALES OFFICES

CDNA04742ENC